AD_____

Award Number: W81XWH-11-1-0306

TITLE: Center for Advanced Bioengineering for Soldier Survivability

PRINCIPAL INVESTIGATOR: Barbara D. Boyan, PhD

CONTRACTING ORGANIZATION: Georgia Tech Research Corporation

REPORT DATE: June 2012

TYPE OF REPORT: Annual

PREPARED FOR: U.S. Army Medical Research and Materiel Command
Fort Detrick, Maryland 21702-5012

DISTRIBUTION STATEMENT: Approved for Public Release;
Distribution Unlimited

REPORT DOCUMENTATION PAGE

Form Approved
OMB No. 0704-0188

1. REPORT DATE *(DD-MM-YYYY)*	2. REPORT TYPE	3. DATES COVERED *(From - To)*
June 2012	Annual Report	23 May 2011 - 22 May 2012

4. TITLE AND SUBTITLE

Center for Advanced Bioengineering for Soldier Survivability

5a. CONTRACT NUMBER

5b. GRANT NUMBER
W81XWH-11-1-0306

5c. PROGRAM ELEMENT NUMBER

6. AUTHOR(S)
Barbara D. Boyan, PhD (PI); Robert E. Guldberg, PhD (Co-PI)

5d. PROJECT NUMBER
10188001

5e. TASK NUMBER

5f. WORK UNIT NUMBER

7. PERFORMING ORGANIZATION NAME(S) AND ADDRESS(ES)
Georgia Tech Research Corporation

Atlanta, GA 30332-0420

8. PERFORMING ORGANIZATION REPORT NUMBER

9. SPONSORING / MONITORING AGENCY NAME(S) AND ADDRESS(ES)
: U.S. Army Medical Research and Materiel Command
Fort Detrick, Maryland 21702-5012

10. SPONSOR/MONITOR'S ACRONYM(S)

11. SPONSOR/MONITOR'S REPORT NUMBER(S)

12. DISTRIBUTION / AVAILABILITY STATEMENT **Approved for Public Release; Distribution Unlimited**

13. SUPPLEMENTARY NOTES

14. ABSTRACT

Our goal is to use advanced bioengineering to develop technologies that will facilitate the transfer of research in musculoskeletal biology and regenerative medicine to patient care. While much is known about the basic biology of cells in the musculoskeletal system, efforts to convert this information to useful products have been limited. This is in part because the technology development teams have failed to include clinicians and engineers collaborating to ensure that the outcomes have clinical utility and the devices can be fabricated and delivered appropriately for medical applications. In addition industry involvement has typically occurred late in the technology development cycle, often requiring re-engineering before inventions can be incorporated into existing products. To avoid these pitfalls, investigators in the Center for Advanced Bioengineering for Solider Survivability will work in teams that include a clinician with experience in military medicine bioengineers, and bioscientists with experience working closely with industry, and wherever possible, an industry partner committed to rapid transfer of the novel technologies. Our over-arching hypothesis is that if technology is developed in this manner, it will move quickly to commercialization in a form that has clinical usefulness.

15. SUBJECT TERMS
Technologies; trauma; bone repair; bioengineering; preclinical models; adult stem cells; translational research.

16. SECURITY CLASSIFICATION OF:			17. LIMITATION OF ABSTRACT: SAR	18. NUMBER OF PAGES	19a. NAME OF RESPONSIBLE PERSON
a. REPORT	b. ABSTRACT	c. THIS PAGE			Barbara D. Boyan, PhD
					19b. TELEPHONE NUMBER *(include area code)* 404-385-4108

Table of Contents

INTRODUCTION

Background: Combat casualty care begins at the front lines of battle and continues into rehabilitation. Current experiences in trauma care in Iraq and Afghanistan have highlighted some critical issues in combat care including the effectiveness and shelf life of blood products, the reduction of wound infections and the reconstruction of bone, tissue and facial structures. Army surgical research concentrates on issues such as hemostasis, resuscitation, bone tissue injury, soft tissue injury, trauma informatics, and clinical trauma. These six areas focus on saving the soldiers' lives, preventing viable tissue loss, and returning the soldiers back to duty as soon as medically possible.

Objective: Our goal is to use advanced bioengineering to develop technologies that will facilitate the transfer of research in musculoskeletal biology and regenerative medicine to patient care. While much is known about the basic biology of cells in the musculoskeletal system, efforts to convert this information to useful products have been limited. This is in part because the technology development teams have failed to include clinicians and engineers collaborating to ensure that the outcomes have clinical utility and the devices can be fabricated and delivered appropriately for medical applications. In addition industry involvement has typically occurred late in the technology development cycle, often requiring re-engineering before inventions can be incorporated into existing products. To avoid these pitfalls, investigators in the Center for Advanced Bioengineering for Solider Survivability work in teams that include a clinician with experience in military medicine, bioengineers, and bioscientists with experience working closely with industry, and wherever possible, an industry partner committed to rapid transfer of the novel technologies. Our over-arching hypothesis is that if technology is developed in this manner, it will move quickly to commercialization in a form that has clinical usefulness.

Study Design: The initial problem addressed in the Center was the need for enabling technologies for reconstruction of bone and facial structures. These are composite tissues consisting of multiple components including nerve, a vascular supply, and at least one or more cell types. We have focused on three technology platforms: imaging of tissues following trauma and during healing; percutaneous stem cell delivery methods; and "smart" scaffolds to promote composite tissue repair. Of particular concern is the interaction of cells with materials and how to optimize this interaction. To achieve these goals our aims are to: (1) establish a translational research center focused specifically on enabling technologies for treatment of composite tissue injuries; (2) develop enabling technologies for delivery of musculoskeletal stem cells; (3) develop enabling technologies for intra-operative deliver of musculoskeletal stem cells in nanofiber mesh wound dressings; and (4) develop technologies for visualizing and controlling internal bleeding and scar formation. Successful attainment of these aims has been facilitated by two advisory boards: a Clinical Advisory Board consisting of surgeons with combat experience, and an Industry Advisory Board that includes senior executives from medical device companies. The achievement of these aims will move our technologies more quickly to large animal models and to the clinic (optional appropriation year).

BODY

Comments on Administrative and Logistical Matters'

During this first month of this grant we set up all internal seed grant accounts and started the IACUC/ACURO and IRB/HRPO application process. We also worked on transferring the ACURO's and HRPO from our FY2008 appropriation to this current one. Due to delays in receiving the notice of award for this grant, the first quarterly report only reported the first month of funding (May 24th -June 30th, 2011). We also initiated the subcontract agreement with the

Queensland University in Australia to test one of CABSS musculoskeletal technologies in a large animal model. The Australian Research Council is sponsoring this study and CABSS has sponsored the surgical supplies being used. No CABSS funds are used for animal purchase or per diem.

Research Proposals

During this year we submitted three AFIRM II proposals (Composite Injury Mode, PI Guldberg; Osteoarthritis Technology, PI Guldberg; and Muscle Regeneration Technology, PI Boyan) as well as three DOD proposals (Wound Care, PI Boyan; Breast Cancer Targets, PI Boyan; and Chondral Lesions, PI Boyan). We had previously awarded four targeted seed grants for projects studying wound healing, internal bleeding and musculoskeletal trauma and several of the seed grants were developed in these proposals.

Importantly, CABSS investigators were awarded a P50 grant from the FDA to establish the Atlanta Pediatric Device Consortium (APDC), which has the purpose of developing and commercializing devices for the pediatric population (age 21 years and younger). This provides CABSS with a route through the product development pathway and enhances our technologies that address the wounded warriors between the ages of 18 and 21.

In addition, a CABSS member company, SpherIngenics, Inc., was awarded an SBIR Phase II grant to develop CABSS technology for craniofacial cartilage regeneration.

CABSS Retreat

During this year we held our annual CABSS Retreat. The CABSS Retreat consisted of the advisory board, CABSS investigators, GT faculty and graduate students. Attached are the minutes of this year's retreat.

The Advisory Board feedback is below:

1. Are the problems we are addressing relevant to military medical problems?

The advisory board agreed that CABSS is addressing medical problems relevant to the military.

2. Is our distribution of resources between discovery, early basic research, and translational research appropriate?

Maribel Baker will send a breakdown of the budgets and how much we are spending on each project. The advisory board suggested using the TRL metric to see how far along a project is and if it's going to be commercializable. Michael Romanko will be sending these metrics to Barbara Boyan.

3. Could we adapt our technology platforms to address emerging medical concerns for the military?

The advisory board suggested using the animal models that CABSS currently has and focus on using them to translate technologies rather than investing more funds in new models.

CABSS had a meeting with SJTRI to discuss standardizing the animal models to be used for industry. SJTRI will apply for ASTM standards, and they are willing to give us 50% of the profit they made on using these animal models.

The advisory board sees the osteoarthritis project as very interesting. This will be a long term 10-15 year project. CABSS should concentrate on preventive technologies for osteoarthritis. Drs. Boyan and Guldberg have developed an OA program, which they submitted to ISR for consideration for funding.

The advisory board was very enthusiastic over the superhydrophobic coating project. There are several other medical applications that can benefit from this coating. The inventors have since filed a patent application and have applied for extramural funding for this project.

Next year, the advisory board would like to see the TRL track system ahead of time to discuss the results during the CABSS meeting.

<u>New Project Initiation</u>

We would like to include a new project on this grant to start on year 2, entitled: "Development of Decellularized Skeletal Muscle Grafts for Limb Reconstruction." The overall objective is to develop and test regenerative technologies that will enable the restoration of muscle function following soft tissue trauma to the limb. A number of strategies have been tested for this purpose with limited success. Reasons for this include failure to re-establish a viable syncitium of myoblasts and failure to form a functional vasculature. Muscle derived stem cells (MDSCs) have been shown to stimulate endogenous healing of existing muscle, but they do not become engrafted, and for large defects may not be practical. Polymer scaffolds have been tested in muscle with similar results. Recent reports showing that decellularized heart tissue can be repopulated with mesenchymal stem cells (MSCs), restoring cardiac function [1], suggest that decellularized cadaver skeletal muscle may be used effectively to restore skeletal muscle.

We will investigate the feasibility of replacing injured or otherwise abnormal muscle with decellularized muscle. The studies described below will use a rat model to screen different graft strategies. We hypothesize that the decellularized muscle will act as a scaffold for the ingrowth of new, healthy muscle in the recipient rat. We also hypothesize that by using this decellularized material as a scaffold, implantation of the material with MSCs will accelerate the healing and improve function. If successful, this experiment will serve as an important step toward the replacement of muscle in humans.

This project will be under Specific Aim 7. The following tasks will be included under this aim:

Task 1. Obtain IACUC and ACURO approvals for the rat model to test different grafts.

Task 2. Determine optimal processing of decellularized muscle grafts to retain three dimensional tissue architecture and tensile strength and provide suture sites at each end.

Task 3. Use a rodent model for screening the effectiveness of decellularized muscle grafts in vivo in order to determine if decellularized muscle grafts will restore muscle structure and function.

Task 4. Determine if addition of MSCs or ASCs will improve graft effectiveness.

The second project is entitled: "Characterization of *in vivo* safety of fibrin-microgel hybrids." This second generation fibrin-binding microgel technologies will utilize single chain human domain antibodies (DAbs) that specifically bind to fibrin, and not fibrinogen, for engagement of fibrin matrices. It is currently unknown how fibrin-binding DAbs or DAb-microgels behave *in vivo*, therefore it is necessary to explore potential complications associated with this technology such as initiation and/or augmentation of thrombi in the body. Because these DAbs have the

potential to interact with endogenous fibrin, it is critical to determine if fibrin-binding DAbs or DAb-functionalized microgels will induce thrombus formation or augment thrombus growth leading to potential stroke and/or heart attack. To this end, we will perform a series of animal experiments to characterize the behavior of DAbs or Dab-microgels in a complex *in vivo* environment. We will use an *in vivo* rat pulmonary embolism model to evaluate the interactions of DAbs and DAb-microgels with endogenous regions of fibrin deposition. In these studies we will evaluate the circulation half-life of the DAbs and DAb-microgels in normal rats and monitor the biodistribution DAbs and DAb-microgels in both normal and embolitic rats.

The pulmonary embolism model utilized for these studies is based on a previously established model that systemically introduces microemboli (2-5μm clot particles) via tail vein injection. The fibrin-binding DAb will be appropriately labeled for near-IR imaging and conjugated to PEG or microgels, then a number of experiments will be pursued to characterize the DAbs.

• Circulation half-life – In these experiments, DAb will be injected via tail vein in normal rats. This will be performed for fibrin-binding DAbs conjugated with PEG of molecular weights of 20, 30 and 40k or pNIPAM-microgels. Blood samples will be collected at 5 min, 30 min, 1 h, 1.5 h, 2 h, 4 h and 24 h after injection and the DAb quantified using a fibrin ELISA and detection of the myc-tag encoded within the ligand.

•Biodistribution – Biodistribution experiments will be performed in both normal and embolized rats. The fibrin-binding DAb or Dab-microgels will be administered via tail vein injection to both embolized and normal rats and anesthetized animals will be imaged in a Fluorescence Molecular Tomography (FMT) system to monitor location of the DAb. After imaging, the animals will be euthanized and organs separated, formalin fixed and sectioned. Sections will be imaged with a Li-Cor near-IR scanner and stained with an anti-myc antibody for the probe to confirm their co-localization with the near-IR probe. Additionally, sections will be stained with the MSB (Martius, Scarlet, Blue) fibrin stain to determine if DAbs or DAb-microgels induce additional thrombin formation and/or augment thrombus growth.

The goal of these studies is to obtain gain an initial understanding of the behavior of fibrin-binding DAbs and DAb-microgels in the presence of endogenous fibrin deposits. This goal will be completed through the following tasks:

This project is tight to Specific Aim 3. The additional tasks will be the following:

Task 11: Apply for IACUC and ACURO approval
Task 12: Develop animal model
Task 13: Perform circulation time studies
Task 14: Perform biodistribution studies

Key Research Accomplishments

The following tasks were targeted this past year:

Specific Aim 1. Expand the translational research center in concert with the External Advisory Board recommendations to include technologies for reconstruction of oral and maxillofacial tissues, detecting internal injuries and treating skin wounds to limit scar formation (CABSS Administration).

Task 1. Review progress in context of new developments in the field and solicit proposals.

Task 2. Establish review criteria to include technology development plan.

Task 3. Identify industry sponsors for joint development projects.

Task 4. Monitor progress toward goals.

Task 5. Develop relevant animal model standards (ASTM and ISO) for testing novel technologies.

Specific Aim 2. Adapt microCT imaging technology for detecting internal bleeding following traumatic injury.

Task 1. Obtain IACUC and ACURO approvals for rodent models of traumatic internal bleeding.

Task 2. Perform femoral artery injury model.

Specific Aim 3. Adapt 3D scaffold and stem cell technology to enhance healing and control scar formation.

Task 1: Obtain all necessary IACUC and ACURO approvals for critical sized full thickness dermal excisional wound models in C57Bl/6J mice.

Task 2: Design and create core shell microparticles that display fibrin 'knobs' homogenously, as an interior shell, and on the outer surface.

Task 3: Characterize the fibrinogen-induced polymerization of the three core shell microparticle variants with 'knob'-presenting linear polymers.

Task 4: Perform in vitro studies to characterize cellular invasion and differentiation within synthetic provisional matrices.

Task 6: Determine the appropriate conditions for large-scale culture, decellularization, and lyophilization, of stem cell embryoid body (EB) extracellular matrices (ECM).

Specific Aim 4. Adapt percutaneous stem cell delivery strategies for craniofacial cartilage defect repair.

Task 1. Characterize rat ear and nasal chondrocytes with respect to extracellular matrix production at the mRNA and protein levels and as a function of passage number.

Task 2. Characterize human auricular and nasal chondrocytes with respect to extracellular matrix production at the mRNA and protein levels and as a function of passage number.

Task 3. Optimize protocol for inducing rat ASCs to express a hyaline cartilage phenotype.

Task 4. Apply for ACURO approval for the rat xyphoid and rabbit implantation models.

Task 5. Apply for IRB/HRPO approval for use of human ear and nose cartilage cells.

Task 6. Perform rat xyphoid defect study for microencapsulated rat ASCs and prechondrocytes.

Task 7. Complete optimization protocols for rat and human ASCs and induced chondrocytes (prechondrocytes) by assessing the viability and phenotype of ASCs and prechondrocytes loaded on silk nanofiber meshes.

Specific Aim 5. Develop graft technologies for palate reconstruction.

Task 1. Obtain IACUC and ACURO approvals for a nude rat palate repair model.

Task 2. Develop methods for decellularizing human palate tissue.

Task 3. Develop methods for loading decellularized human palate tissue with ASCs (without microbeads and with microbeads).

Specific Aim 6. Adapt stem cell delivery technology for treatment of large bone defects.

Task 1. Obtain IACUC and ACURO approval for use of human stem cells on fiber mesh scaffolds in critical size defects in the rat.

Task 2. Obtain IRB/HRPO approval for obtaining human ASCs.

Task 3. Determine if human ASCs are viable in microbeads and assess their osteogenic differentiation potential and growth factor release.

The following was accomplished this past year:

Specific Aim 1. Expand the translational research center in concert with the External Advisory Board recommendations to include technologies for reconstruction of oral and maxillofacial tissues, detecting internal injuries and treating skin wounds to limit scar formation (CABSS Administration).

Task 1. Review progress in context of new developments in the field and solicit proposals.

Q1: We have identified three seed projects, which were funded as a result of this continuation grant. In addition, we solicited proposals from Georgia Tech faculty for a related seed grant program with the purpose of developing technologies with high impact potential. One of these projects, "Biocompatibility of Superhydrophobic Coated Polymers for Biomedical Applications" will develop technologies for preventing biofilm formation on polymeric devices such as catheters, wound dressings, and percutaneous implants. We are quite excited about this technology and are considering bringing it into the CABSS program.

Task 2. Establish review criteria to include technology development plan.

Q1: One of our main goals is to identify technologies that can be commercialized for clinical use. We have been working with our investigators to identify promising technologies with this potential. Our team of company advisors is helping us establish review criteria for this purpose.

Task 3. Identify industry sponsors for joint development projects.

Q1: CABSS is working together with the Translational Research Institute for Biomedical Engineering and Science (TRIBES) to bring companies to Georgia Tech to showcase early development technologies. The goal is to promote industry research sponsorship early on to translate technologies faster. To date, we have had visits from two companies, KCI and KLS Martin. We are working to continue this partnership and we are planning on bringing several other companies throughout the year.

Task 4. Monitor progress toward goals.

Quarterly Reports will be used to monitor progress of each seed grant project. Each seed grant PI will present during the annual CABSS retreat and the external advisory board will decide if funding should be renewed or terminated depending on their progress.

Task 5. Develop relevant animal model standards (ASTM and ISO) for testing novel technologies.

We are developing five new animal models for screening novel technologies:

1. Rat model of osteoarthritis.
2. Rat composite injury model.
3. Rat muscle repair model.
4. Sinus lift model for assessing bone graft materials.
5. Use of a novel snake algorithm for monitoring nonunion formation.

Specific Aim 2. Adapt microCT imaging technology for detecting internal bleeding following traumatic injury.

Task 1. Obtain IACUC and ACURO approvals for rodent models of traumatic internal bleeding.

We applied and obtained approval for IACUC and ACURO for detecting internal bleeding following traumatic injury. The ACURO approval # 10188001.01 was obtained June 02, 2011. The approval letter is attached.

Task 2. Perform femoral artery injury model.

Over the past year, we have continued to develop and analyze the intracerebral hemorrhage (ICH) model which will be utilized to test the use of microCT to non-invasively detect internal bleeding. Over the past year, we have continued to develop and analyze the intracerebral hemorrhage (ICH) model which will be utilized to test the use of microCT to non-invasively detect internal bleeding. We have successfully verified our ability to achieve reproducible injuries within rats using an intracerebral injection of bacterial collagenase (Fig.1). Through histological analysis, we have confirmed the influx of red blood cells into healthy brain tissue within the left hemisphere approximately 1.5 hours after the stereotaxic injection of collagenase (Fig. 2). Over the past year, we have performed additional histology to locate the presence of IgG within the brain after ICH (Fig. 2B). This technique will facilitate quantification of the extent of injury within the brain which can be compared to data obtained from CT imaging.

We have also conducted additional imaging studies which indicate superior contrast at the injury site resulting from the administration of liposome encapsulated contrast agent compared to free contrast agent (Fig. 3). MicroCT images were obtained 1 hour after administration of collagenase. Intravenous administration of free contrast agent (2g/kg iodine) did not result in contrast enhancement at the site of injury (Fig. 3A-C); however, the injury site can be detected when liposomal contrast agent is utilized (Fig. 3D-F). Additional imaging studies are currently underway to verify these preliminary results, and image quantification methods are being developed to enable statistical evaluation of the data.

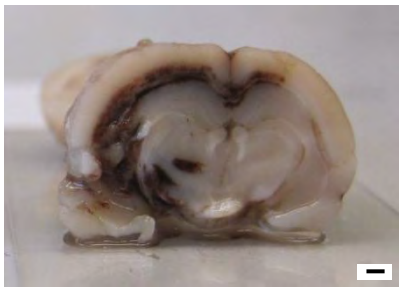

Figure 1. Transverse view of rat brain 1.5 hours after intracerebral administration of collagenase into the left hemisphere. Scale bar is 1mm.

.

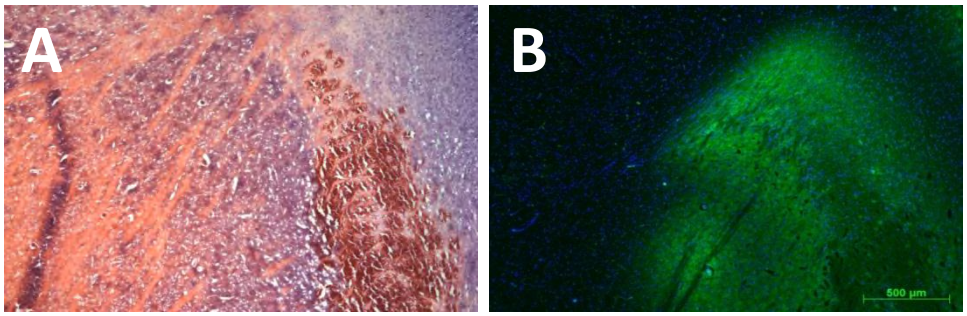

Figure 2. Histological analysis of intracerebral hemorrhage model. Brains explanted from rats subjected to collagenase treatment were sliced into 14um sections. A) Sections were stained with hematoxylin and eosin, which demonstrated an influx of red blood cells. B) Staining of an adjacent section with an antibody to rat IgG (green) present in the bloodstream verified this result. Nuclei were stained with DAPI (blue). Scale bar is 500um.

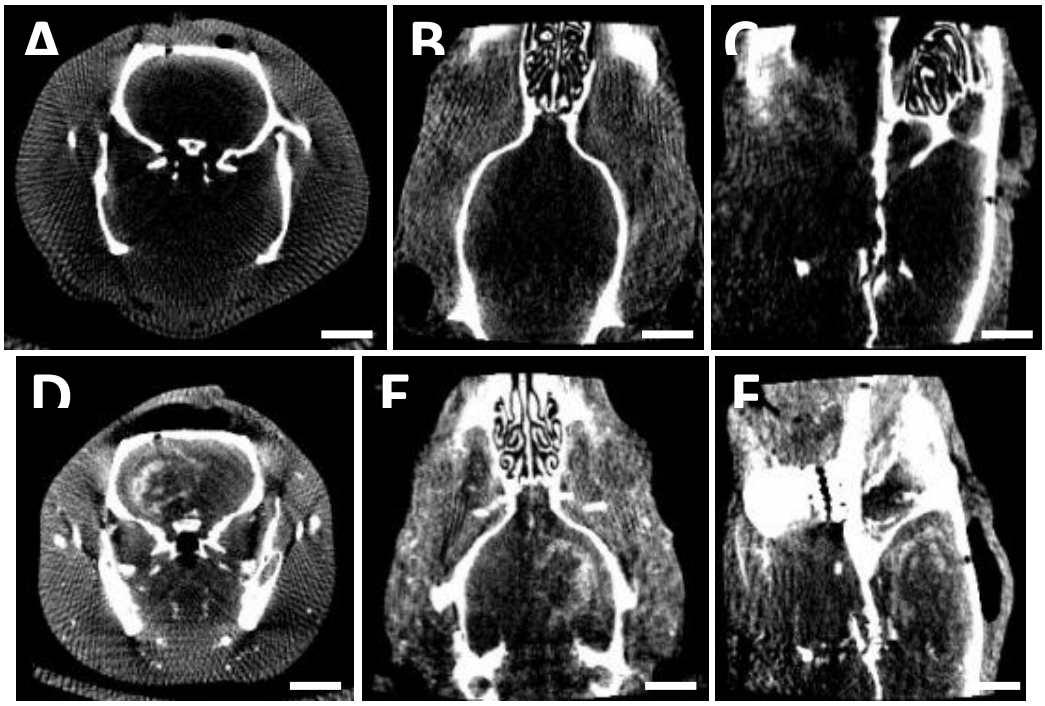

Figure 3. MicroCT images of ICH rat brains. Axial (A, D), coronal (B, E), and sagittal (C, F) views of injured rat brains after intravenous administration of free (A-C) or liposomal (D-F) contrast agent. Images were acquired 1.5 hours after intracerebral administration of collagenase into the left hemisphere. Enhanced contrast is apparent at the injury site directly below the burr hole in the skull for animals receiving liposomal contrast; whereas administration of free contrast agent did not result in contrast enhancement. Scale bar is 5mm.

Specific Aim 3. Adapt 3D scaffold and stem cell technology to enhance healing and control scar formation.

Task 1: Obtain all necessary IACUC and ACURO approvals for critical sized full thickness dermal excisional wound models in C57Bl/6J mice.

We received IACUC approval from Georgia Tech on this protocol. We are working on the ACURO application. No animal studies have been done.

Task 2: Design and create core shell microparticles that display fibrin 'knobs' homogenously, as an interior shell, and on the outer surface.

pNIPAm Microgel Synthesis: pNIPAm microgel particles were synthesized by free-radical precipitation polymerization. Copolymerization with AAc was done to allow for chemoligation sites for peptide attachment. Reaction conditions were used that favor chain transfer reactions at the polymer backbone which lead to cross-linking reactions without the need for additional cross-linking monomers. The microgels were lyophilized until further use. Monodispersity and hydrodynamic radius of the microgels was determined using dynamic light scattering (DLS).

Fibrin Knob Peptide Conjugation to Microgels: Fibrin knob peptides (GPRPFPAC- MW: 844g/mol and GPSPFPAC-MW: 774.89g/mol) were purchased from GenScript Corp (Piscataway, NJ). Peptide conjugation to the pNIPAm microgels was done using a two step conjugation method. As previously described in the microgel synthesis, the carboxyl groups were introduced through the copolymerization of AAc (5% molar ratio). The fibrin knob peptides were then conjugated to the microgels using maleimide coupling to the free cysteine residues on the C-termini of the peptides.

Peptide coupling was done using a proprietary method developed in our lab. Excess unconjugated peptide was removed from the peptide-functionalized microgels using flow through microdialysis with a 10kDa filter membrane and purified 5X into dH_2O, then lyophilized.

Table 1. DLS of pNIPAm +5% AAc microgels showing hydrodynamic radius and polydispersity index.

DLS Results Summary:	Radius (nm)	Polyd Index
	474.1	0.07

The DLS results show a microgel diameter of approximately 1um, and a polydispersity index below 0.1 indicates monodisperse particles.

The microgel concentration in the bioconjugation reaction was estimated to be 1.28mg/ml, and the peptide concentration in the reaction was estimated to be 0.567mM. To reflect similar concentrations, all unconjugated microgel controls were at 1.28mg/ml, and all free peptide controls were at 0.5mM. The results of the assay show that the peptides react with the maleimide functionalized microgels almost instantaneously after being added to solution, but do not react with unconjugated microgels, indicating that the bioconjugation reaction is a specific reaction carried out to completion very rapidly.

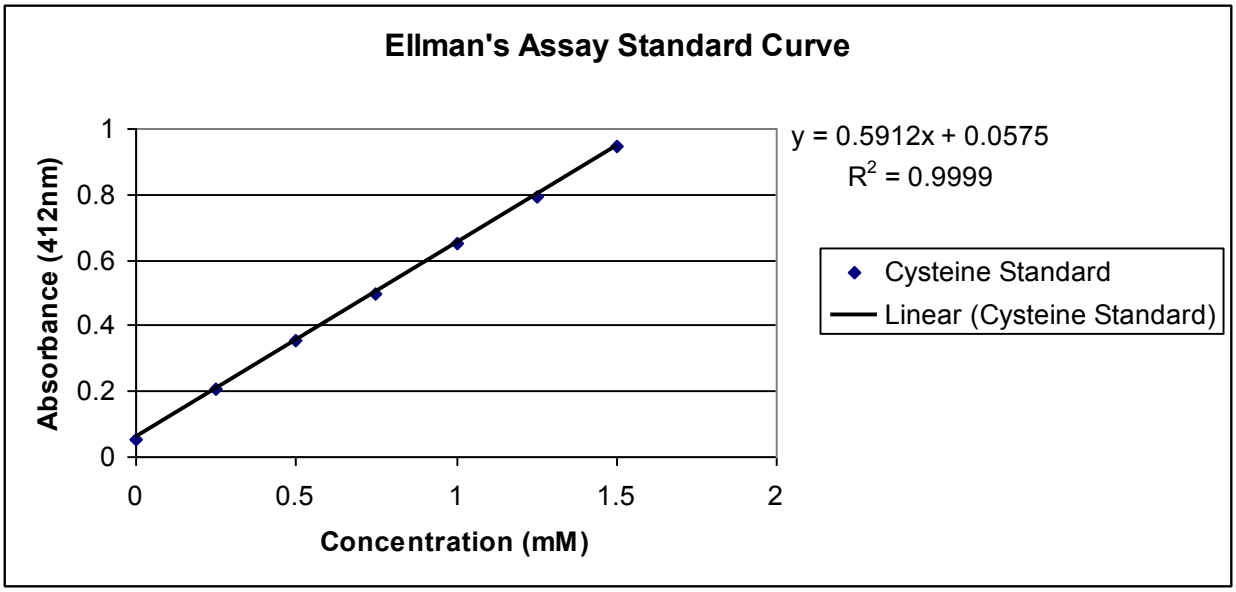

Figure 4. Ellman's assay standard curve generated using cysteine standards.

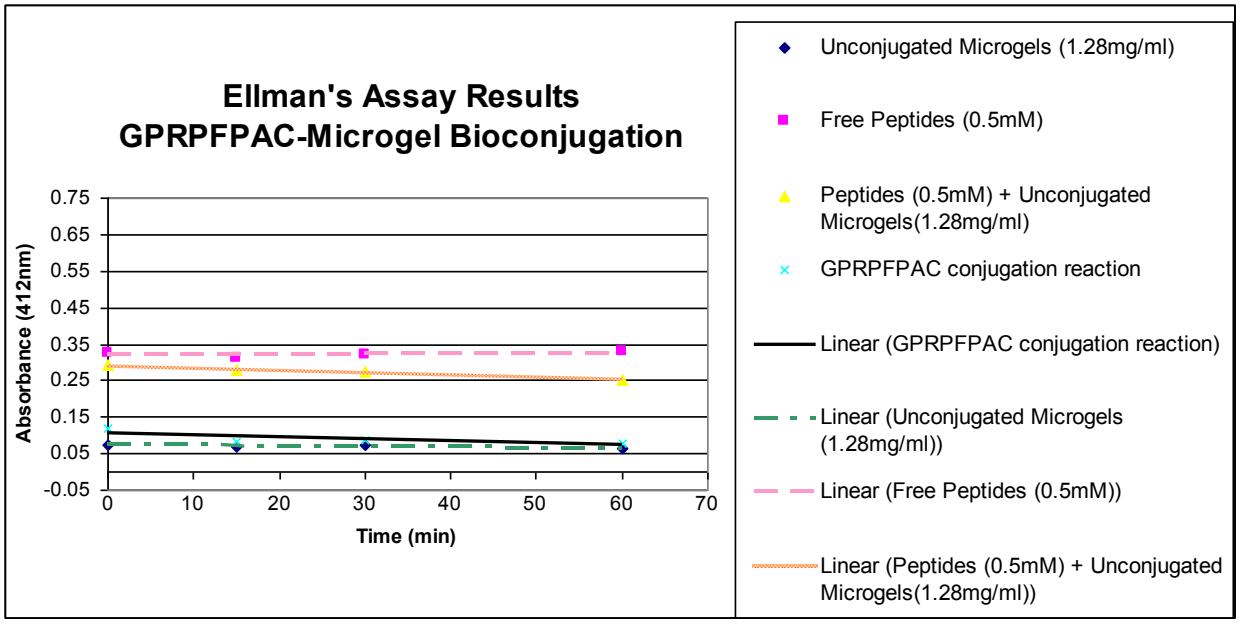

Figure 5. Ellman's assay results for GPRPFPAC-microgel bioconjugation.

Below is an update of the following tasks:

Task 3: Characterize the fibrinogen-induced polymerization of the three core shell microparticle variants with 'knob'-presenting linear polymers.

Task 4: Perform in vitro studies to characterize cellular invasion and differentiation within synthetic provisional matrices.

Fibrin polymerization and network structure are dependent upon fibrinogen, thrombin, and calcium concentration. The addition of fibrin knob peptide labeled microgels in a fibrin network is expected to alter network formation and the final structure of a fibrin clot.

Following the synthesis of fibrin knob peptide labeled microgels, the influence of these microgels on clot formation and final clot structure were explored this past year and the results are shown in the following section.

Fibrin polymerization in the presence of fibrin knob peptide labeled microgels

The conversion of fibrinogen into fibrin fibers causes an increase in clot turbidity, and fibrin network formation was observed by measuring the change in clot turbidity upon the addition of thrombin (fibrinogen clotting enzyme) to a solution of fibrinogen. Thrombin catalyzed polymerization of mixtures of fibrinogen (1mg/ml) and various fibrin knob peptide labelled microgels [unfunctionalized microgels (1mg/ml), GPRPFPAC-microgels (1mg-ml), and GPSPFPAC-microgels (1mg/ml)] was initiated in 96-well plates. In this assay, thrombin concentration dependent polymerization was observed for fixed concentrations of fibrinogen and microgels. Wells of 90ul of the fibrinogen and microgel mixture were incubated for 2 hours at room temperature.10ul of various concentrations (0, 0.01, 0.025, 0.05, 0.075, 0.1, 0.25, and 0.5 NIH units/ml) of human α-thrombin were added to the fibrinogen-microgel mixtures to initiate polymerization. The clot turbidity at A_{350} was measured for 2 hours using a plate reader, with readings taken every minute. From the turbidity curves, it was possible to determine the final turbidity of the mixture (normalized against controls without thrombin), and the clotting half time- the time taken for the clot to reach half the final turbidity value (at 2hrs following thrombin addition).

Following the turbidity assay, to determine the amount of unclotted protein, the clot was removed, and the isolated clot liquor was analyzed for total soluble protein using the Quant-it Protein Assay (Invitrogen). The %clottable protein was then back calculated from the amount of soluble protein in the clot liquor, normalized against controls without thrombin.

Results

Fibrin polymerization using various concentrations of thrombin was used to generate turbidity profiles for the hybrid fibrin-microgel clots. As expected, the curves progress from a slow and gradual increase in clot turbidity to rapid polymerization and increase in turbidity with higher concentrations of thrombin. Preliminary turbidity results are shown below.

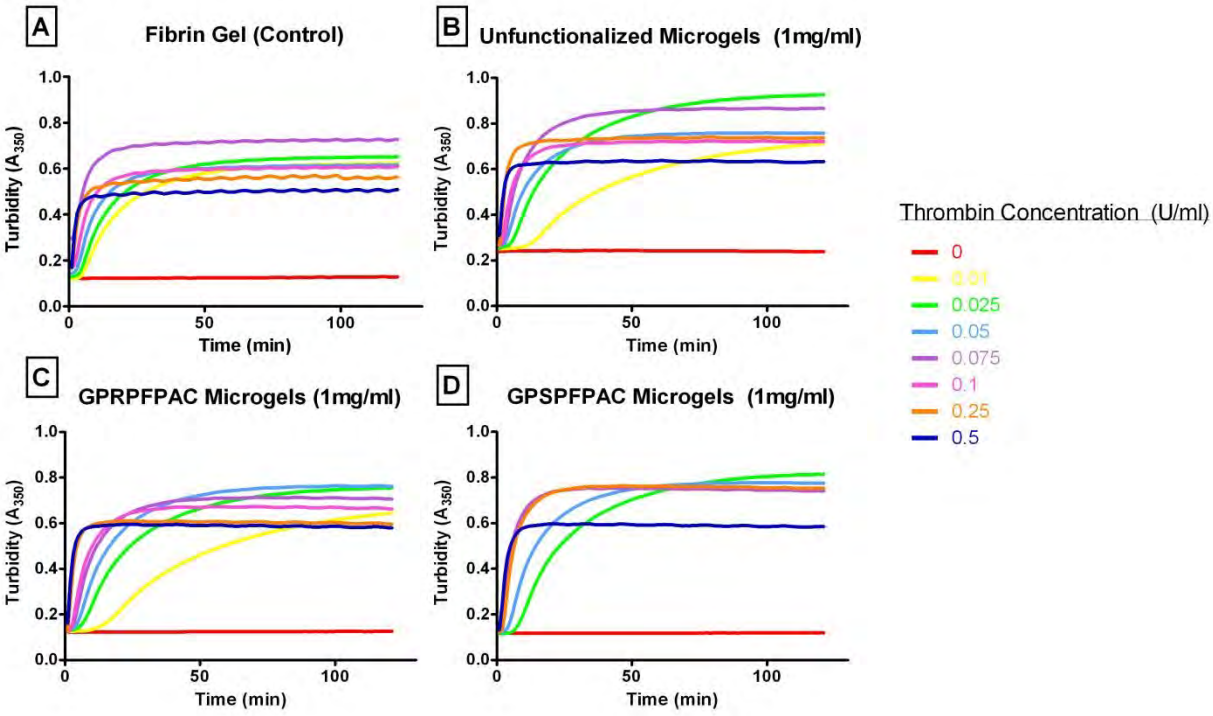

Fig. 6. Fibrin polymerization parameters: 1mg/ml fibrinogen, and 1mg/ml microgels, with thrombin concenrations of 0, 0.01, 0.025, 0.05, 0.075, 0.1, 0.25, 0.5 U/ml. Representative turbidity curves (n=9) for: (A) control (fibrinogen only); (B) 1mg/ml unconjugated microgels; (C) 1mg/ml GPRPFPAC microgels (D) 1mg/ml GPSPFPAC microgels *Data missing for 0.01, and 0.1 U/ml thrombin condition for GPSPFPAC microgels.*

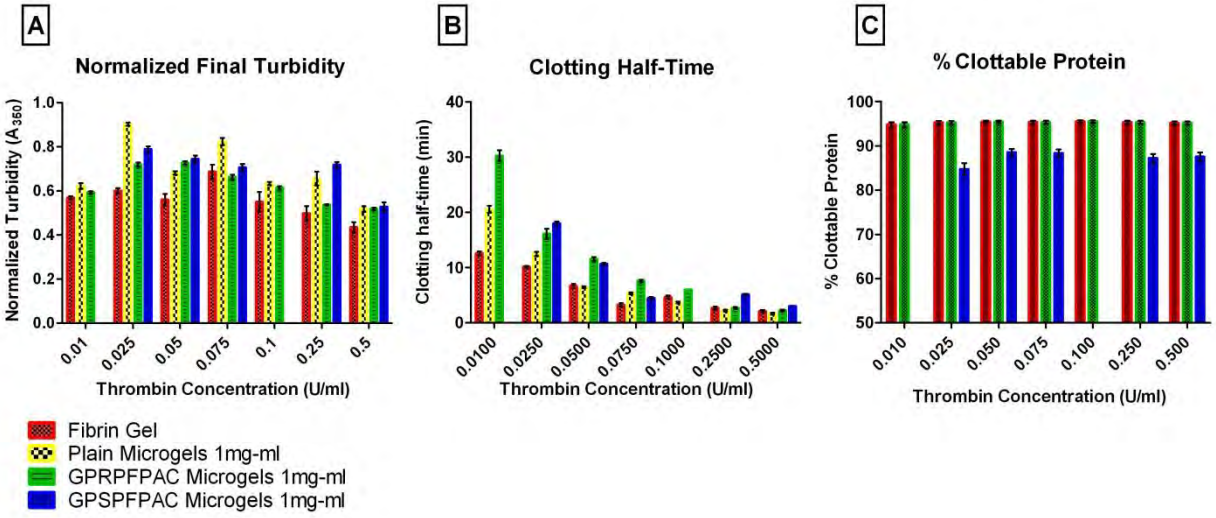

Fig. 7. (A) Absolute final clot turbidity normalized against controls with no thrombin addition. (n=9) (B) Clotting half-times of various fibin-microgel mixtures, calculated from turbidity curves (n=9). (C) Perectage of clottable protein backcalculated from the amount of soluble protein in the remaining clot liquor after clots were removed (n=9) *Missing final turbidity and clotting half-time data for 0.01, and 0.1U/ml thrombin condition for GPSPFPAC microgels and missing %clottable protein data for unlabelled microgels*

Clot turbidity can indicate differences in fibril organization in various compositions of fibrin networks. The addition of microgels to the fibrin network seems to generally increase the final clot turbidity in all the various thrombin conditions, but the reason for this in all clots containing microgels is unknown. The clotting half-time shows a similar trend as the turbidity data, where the lowest thrombin concentrations used to polymerize a clot have the highest clotting times. While the overall clot turbidity seems to increase in the presence of microgels, the addition of microgels at these low thrombin concentrations seems to also increase the clotting half-time. It is possible that the presence of microgels in the mixture provides a physical barrier and hinders fibrin monomer access to other fibrin monomers thereby preventing rapid polymerization of the network. The percent clottable protein in the control for all thrombin conditions is approximately 95%. The GPRPFPAC microgels (1mg/ml) appear to have no significant change in percent clottable protein as the control, but the GPSPFPAC microgels have a slight decrease in the amount of clottable protein.

The results from the turbidity data are inconclusive at this point (see * below). Data from higher concentrations of microgels incorporated in fibrin gel networks is necessary to see if there is a significant difference in the final turbidity, clotting half-time, and percent clottable protein with an increase in fibrin knob peptide functionalized microgels.

Missing turbidity data for 0.01 and 0.1U/ml Thrombin for GPSPFPAC microgels 1mg/ml. Missing %clottable protein data for unfunctionalized microgels. Need these to complete statistical analysis.

Clot structure and morphology: confocal imaging of hybrid fibrin-microgel gels

Clots containing 10% Alexa Fluor 555-labelled fibrinogen were imaged using the Zeiss 510 laser scanning confocal microscope. Mixtures of 10ul fibrinogen and 10ul microgels were preincubated for 1 hour prior to 20ul thrombin addition, for a final concentration of 1mg/ml fibrinogen, 0.25U/ml thrombin, and either 1mg/ml or 5mg/ml microgels. Following the addition of thrombin, the solutions were quickly mixed by pipetting and immediately added to a glass slide. The mixture was covered with a glass coverslip supported by 0.3mm spacers on two sides. The open sides were sealed with nail polish to create a chamber, and the mixture was allowed to polymerize for 1hour before imaging. A 10um Z-stack of 20 (0.5nm) slices under the 63X objective was captured for reconstructing the 3D fibrin network structure. At least 3 clots were formed independently for each condition, and 4 random sections were imaged per clot.

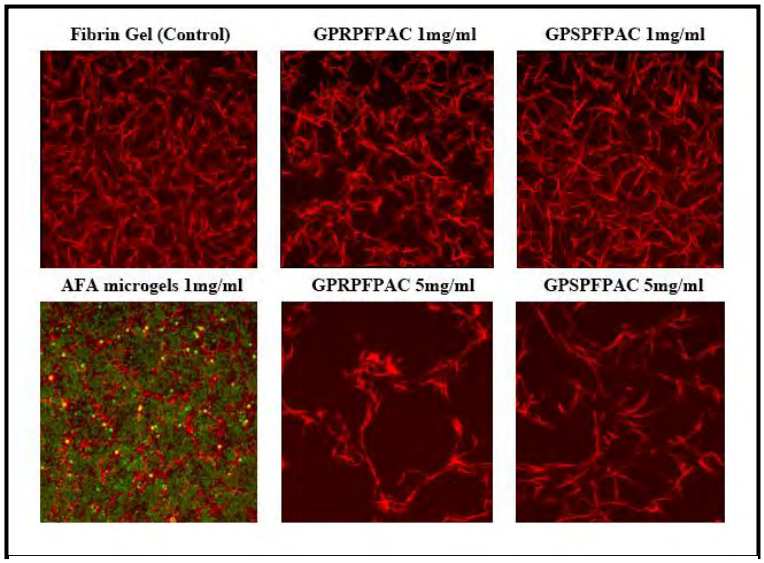

Fig. 8. Representative confocal images of fibrin network structures in the presence of various microgel conjugates (n=12).

In order to visualize the microgels in the fibrin network structure, 0.1M AFA (4-acrylamidofluorescein)-labeled microgels were synthesized using the same method as for unlabelled microgel synthesis (with the addition of 0.1M AFA to the monomer solution prior to initiation).

In order to directly observe the change in network structure upon the addition of various microgel conjugates, clots formed with fluorescently labeled fibrinogen were polymerized on glass slides to enable imaging of the 3D fibrin network using confocal microscopy. Clots were formed using 1mg/ml and 5mg/ml of the fibrin knob peptide labeled microgels. Clots containing 1mg/ml GPRPFPAC microgels had shorter more branched fibers than the fibrin control, and the clots containing 1mg/ml GPSPFPAC microgels had longer thinner fibers, and is more similar in structure to the control. Interestingly, at a higher microgel concentration the clots containing 5mg/ml GPRPFPAC microgel had nodular like structures with a greatly reduced total fiber volume than the control. One possible explanation for the nodular structures is the formation of fibrin-microgel aggregates where the local concentration of GPRPFPAC peptide available for association with fibrin holes is high. The 5mg/ml GPSPFPAC microgel condition had a similar long thin fiber structure as the 1mg/ml sample but with reduced total fiber volume.

The general trend shows that with a higher concentration of microgels there is less total fiber volume. It is suspected that the areas not occupied by the fibers are filled with microgels, but because the peptide labeled microgels are not fluorescently tagged, it is not possible to observe the relative locations of the microgels in conjunction with the fibers. In order to observe the microgels within the fibrin network structure, pNIPAm microgels were synthesized containing 0.1M AFA. Clots containing 1mg/ml AFA-microgels were observed using excitation by the Ar 488 laser, and the labeled fibrinogen was observed using excitation by the He 543 laser under the multitracking mode. It is clear to see that the areas not occupied by the fibrin fibers are filled with microgels.

Further turbidity assays using higher fibrin knob peptide labeled microgels need to be done in order to get a more complete picture of clot formation. The next step in confocal imaging will be to fluorescently label the fibrin knob peptide labeled microgels for a better understanding of fibrin network structure alteration in the presence of peptide labeled microgels. In order to further analyze the clot structure, the mechanical properties of these hybrid fibrin-microgel gels will be probed using microrheology.

The design of microgels that display fibrin knob binding peptides is expected to enhance the hemostatic process and wound healing by altering fibrin network formation and the final structure of a fibrin clot. We have previously shown the synthesis and characterization of fibrin knob peptide labeled microgels as well as preliminary characterization of fibrin network polymerization and structure in the presence of these microgels. Further characterization of fibrin polymerization kinetics and final clot mechanical strength in the presence of fibrin knob peptide labeled microgels are explored in the following section.

Fibrin polymerization kinetics using dynamic light scattering

The formation of fibrin fibers from fibrin monomers and polymerization into a clot causes an increase in the light scattered from the forming fiber network which can be measured by dynamic light scattering. A DynaPro™(Protein Solutions™) Plate Reader DLS was used to measure the change in the scattering intensity upon the addition of thrombin to a fibrinogen/ fibrinogen-microgel solution. The fibrinogen-thrombin solutions were mixed in a 1:1 volume ratio for a final volume of 60ul in a single well in a 384-well black clear bottom plate, for a final fibrinogen concentration of 1mg/mL, and a final thrombin concentration of 0.25U/mL. For samples containing microgels, the final concentration of microgels was 1mg/mL. The scattering intensity was measured by taking measurements for 2500 seconds at 22°C of 1 acquisition each consisting of 20 second reads with 20 reads. After 5 acquisitions to establish a base line scattering of the fibrinogen/ fibrinogen-microgel solution, thrombin was spiked in and the

scattering intensity was measured for the remainder of the experiment. Each sample was measured 3 times (n=3).

Clot mechanical properties: rheology of fibrin-microgel gels

A Physica MCR 501 Rheometer was used to examine the viscoelastic properties of fibrin clots in the presence of microgels. For the fibrin control, the reaction components, fibrinogen and thrombin, were thoroughly mixed with a pipette in a 9:1 volume ratio for a final volume of 200ul, a final fibrinogen concentration of 1mg/mL, and a final thrombin concentration of 0.25U/mL in a 25mM HEPES, 150mM NaCl, and 5mM $CaCl_2$ buffer. For samples containing microgels, the microgels were added to the fibrinogen solution and allowed to incubate at least 1 hour prior to experiments for a final concentration in the total clotting mixture of 1mg/mL. After mixing in the thrombin, 180ul of the clotting mixture was quickly transferred to the center of the bottom plate of a cone-plate fixture set-up (2.014° cone angle, and 24.960mm diameter). The cone was quickly lowered to the measurement position, and the sample was allowed to polymerize at room temperature for 2 hours before taking measurements. In order to prevent evaporation of the sample, dH_2O was applied to a ring surrounding the exposed surfaces of the clots in a humidity chamber surrounding the cone-plate set up.

Measurements were taken in oscillation mode at 0.5% strain for a range of between 0.05 and 50Hz at 6points/decade. The storage modulus (G'), a measure of the elastic energy stored during the deformation imposed by one oscillation of the rheometer, calculated by the Rheoplus software, was used as a measure of clot rigidity. The loss modulus (G"), the energy dissipated by the clot during deformation, was also recorded. Each sample was measured 3 times (n=3).

Fibrin polymerization using various concentrations of thrombin was used to generate turbidity profiles for the hybrid fibrin-microgel clots. The complete experimental data set is included in the results below. The results in Figure 9 show that there is no significant alteration in polymerization time for the microgel containing clots, except for the highest concentration GPRPFPAC microgel containing clots. At low thrombin concentrations, these clots have a delayed polymerization rate as measured by the change in absorbance, but upon reaching thrombin concentrations of 0.1U/mL and above, they exhibit normal clot polymerization behavior. This suggests that at lower concentrations of thrombin there is a competitive effect of the positive binding peptide displaying microgels with the native fibrin monomers for polymerization into a fiber network.

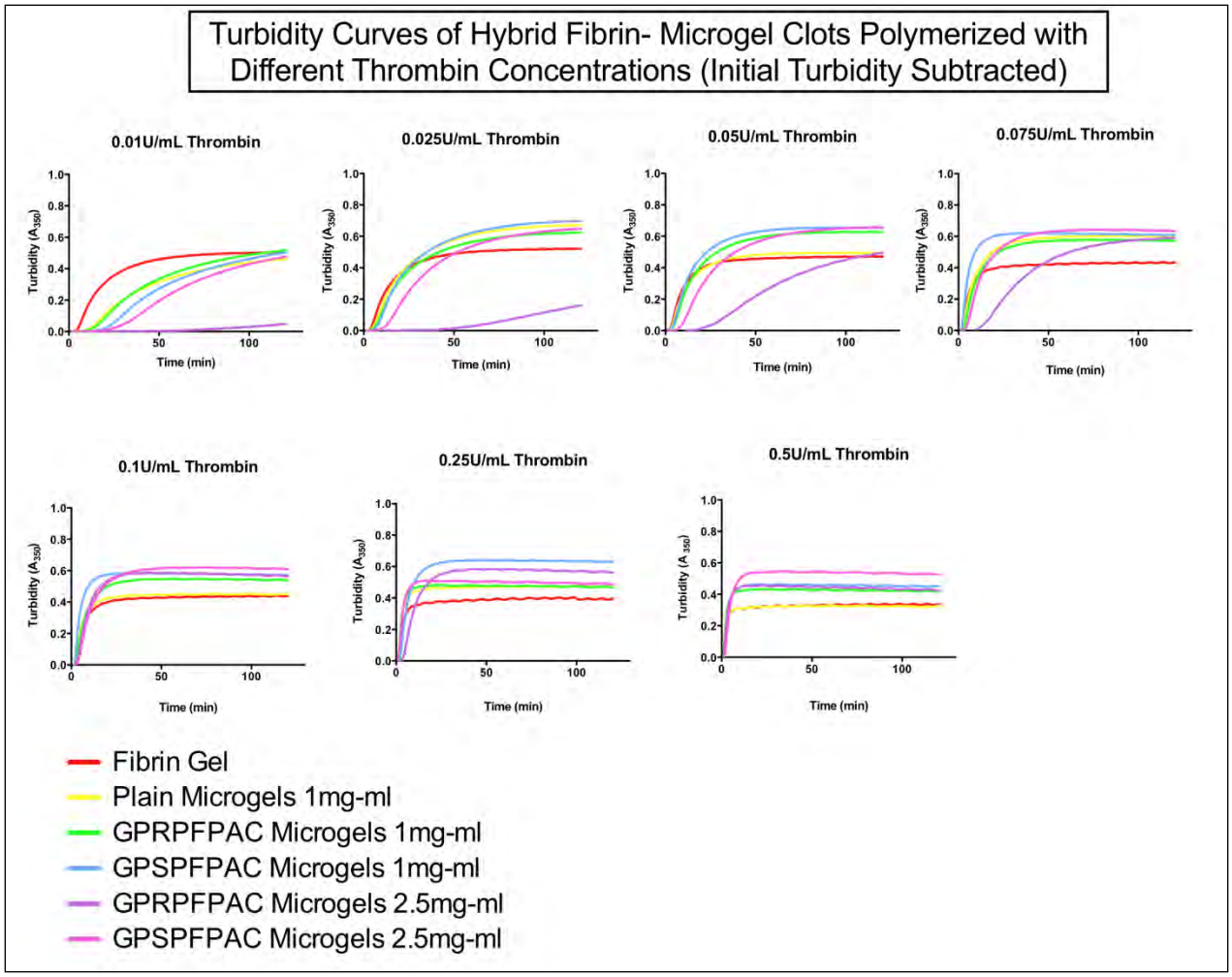

Figure 9. Turbidity profiles of fibrin-microgel clots polymerized using different thrombin concentrations (0.01U/mL – 0.5U/mL).

Except for the 2.5mg/mL GPRPFPAC microgel containing clots, the overall results in Figure 10 show that the final turbidity of microgel containing clots is higher than the fibrin control. However, the clotting half time as defined by the time needed to reach ½ final turbidity at 2 hours, is greater for clots containing higher concentrations of microgels polymerized with low concentrations of thrombin (< 0.1U/mL). This impedance of rapid fiber formation is likely due to the steric hindrance effect of microgels disrupting fibrin monomer or fiber-fiber interaction for network formation. Despite the slower initial polymerization rate, the clots reach the final turbidity value over the course of two hours, and at higher thrombin concentrations (≥0.1U/mL) all of the clots display similar clotting half-times. Similarly, the clots containing higher microgel concentrations polymerized with low concentrations of thrombin (< 0.1U/mL) contain less clotted protein after 2hours of polymerization. The same clots polymerized with higher concentrations of thrombin (≥0.1U/mL) have on average similar amounts of clotted protein with the higher microgel concentration containing clots having slightly less total protein encorporated into the clot due to volume exclusion by the microgels.

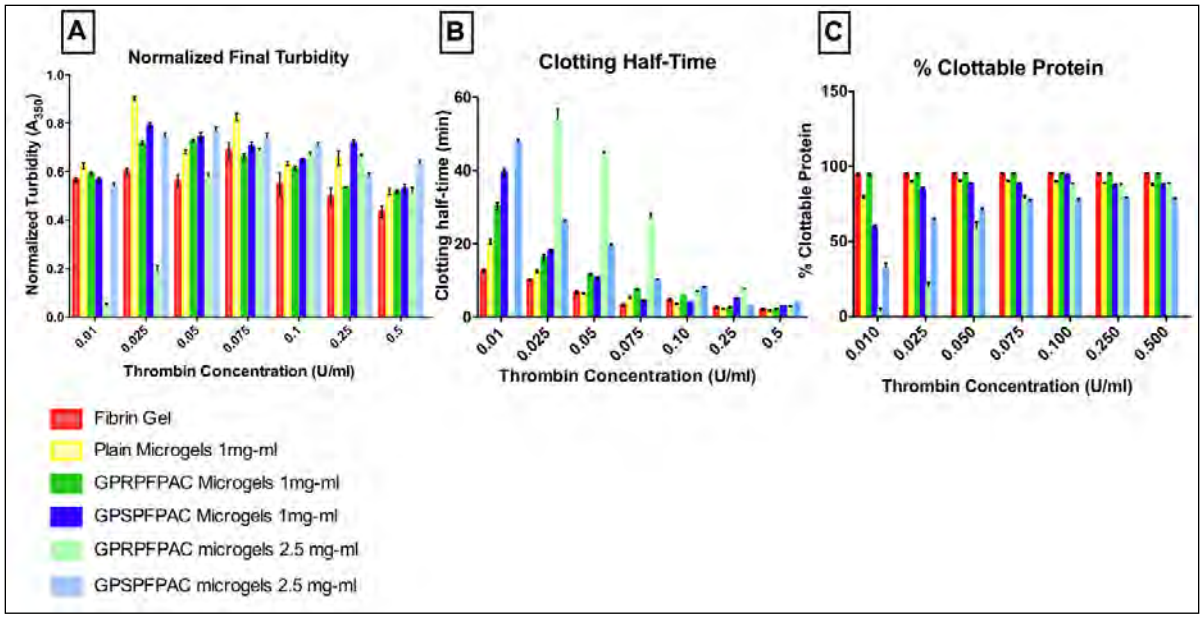

Figure 10. A) Normalized final turbidity of clots after 2 hours polymerization. B) Clotting half-time of clots, defined by the time needed to reach ½ final turbidity at 2 hours. C) %Clottable protein in the clots after 2 hours polymerization.

The dynamic light scattering results show a large increase in the scattering intensity immediately upon addition of thrombin to the solution mixture. There are no significant differences in the scattering intensity curves upon initiation of polymerization between the fibrin control and microgel containing clots as shown by Figure 11.

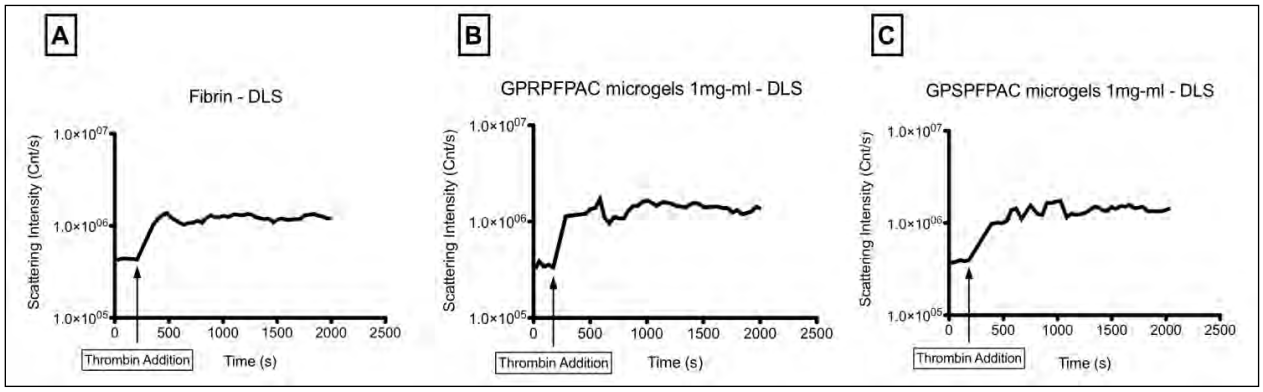

Figure 11. Representative scattering intensity curves of fibrin polymerization upon addition of thrombin. A) Fibrin control. B) Fibrin polymerized in the presence of GPRPFPAC labeled microgels (1mg-ml) C) Fibrin polymerized in the presence of GPSPFPAC labeled microgels (1mg-ml).

The mechanical strength of low fibrinogen concentration containing clots fall within the range of 10s of Pascals, which is considerably low for use in clinical applications. However, with the addition of microgels into the clot structure, the storage modulus increases by almost 4 times the value for a fibrin gel. These results show the potential of fibrin-microgel gels to increase the mechanical strength of the clot even with low protein concentrations while maintaining adequate clot polymerization rates.

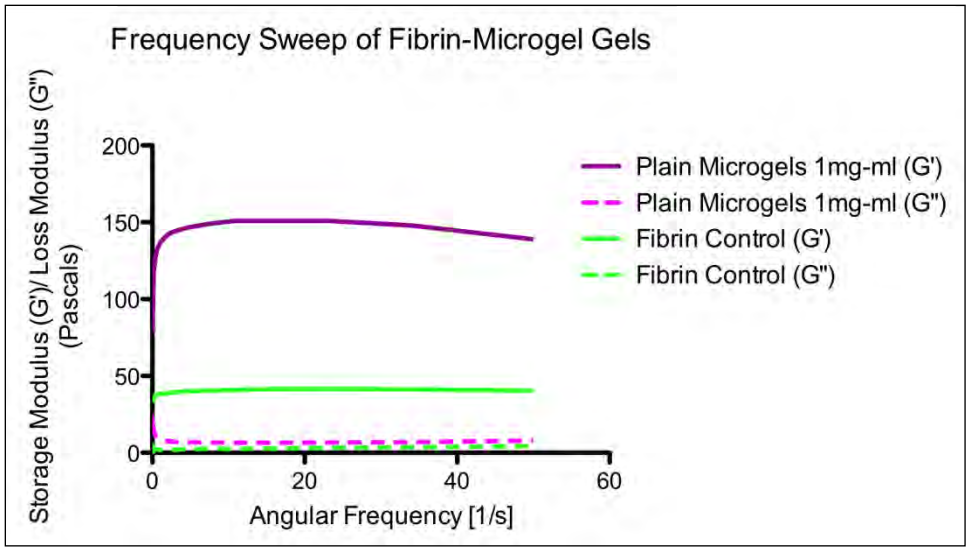

Figure 12. Representative curves of G' and G" of fibrin gel controls and fibrin clots polymerized in the presence of 1mg-ml unfunctionalized microgels.

Further mechanical strength characterization of peptide-labeled microgel containing fibrin clots is underway to determine whether they have an effect on fibrin clot rigidity and strength. Confocal imaging of fibrin clots containing fluorescently labeled peptide-displaying microgels is also in progress to determine the interaction of the peptide-labeled microgels with fibrin fibers. The results so far have shown that the incorporation of microgels and peptide-labeled microgels into a fibrin network alters fibrin structure and clot mechanical properties, but it is important to determine whether these fibrin binding peptide labeled microgels bind to fibrinogen alone. This will be determined using an ELISA plate binding assay. Also the ability of cells to grow and proliferate in this hybrid microgel-fibrin gel as compared to a fibrin clot control will be assessed using an angiogenesis assay.

Hybrid Fibrin-Microgel Clot Mechanical Properties and Cell Incorporation

The behavior of fibrin-microgel clots under shear force and compression was examined by bulk rheology and bulk compression, respectively, in order to determine the effect of microgels on the strength and rigidity of a fibrin matrix. Cells were then incorporated into polymerizing matrices with fibrin and fluorescent microgels.

The stress response of a fibrin-microgel matrix to an oscillatory shear strain in the linear regime was measured using rheology. In the linear regime, for elastic materials the stress is in phase with the strain and the proportionality constant is the elastic modulus of the material ($\sigma=E\gamma$). By contrast, for viscous liquids the stress is out of phase with the strain by $\pi/2$, indicating that the stress is proportional to the strain rate, and the proportionality constant in this case is the viscosity ($\sigma=\eta\gamma'$).

The elastic or in-phase part of the stress is associated to a storage modulus G', while the viscous or out-of-phase part of the stress is associated with a loss modulus G''. The time scale separating the two is the relaxation time (τ), where the crossover between G' and G'' occurs. The influence of microgel-colloidal assemblies within a fibrin matrix on the viscoelastic properties can be assessed by determining the change in the relaxation time due to the incorporation of microgels within a fibrin network

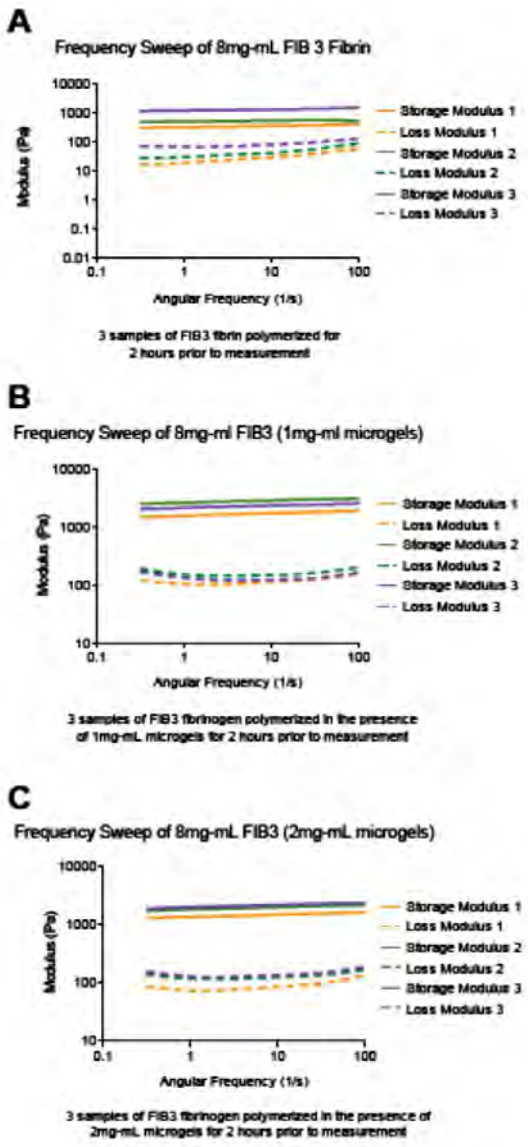

Figure 13. Frequency Sweeps of Fibrin-Microgel Gels. (A) 8mg/mL fibrin control (B) 8mg/mL fibrin + 1mg/mL microgels (C) 8mg/mL fibrin + 2mg/mL microgels.

A Physica MCR 501 rheometer (Anton Paar, Hertford Herts, UK) was used to examine the viscoelastic properties of fibrin clots in the presence of microgels. For the fibrin control, the reaction components, fibrinogen and thrombin, were thoroughly mixed in HEPES +Ca buffer in a 9:1 volume ratio for a final volume of 200ul, a final fibrinogen concentration of 8mg/mL, and a final thrombin concentration of 1U/mL. For samples containing microgels, the microgels were added to the fibrinogen solution and allowed to incubate at least 1 hour prior to experiments for a final concentration in the total clotting mixture of 1 and 2mg/mL. After mixing in the thrombin solution, 180uL of the clotting mixture was quickly transferred to the center of the bottom plate of a cone-plate fixture set-up (2.014° cone angle, and 24.960mm diameter). The cone was quickly lowered to the measurement position, and the sample was allowed to polymerize at room temperature for 2 hours before taking measurements. In order to prevent evaporation of the sample, dH2O was applied to a ring surrounding the exposed surfaces of the clots in a humidity chamber surrounding the cone-plate set up.

Measurements were taken in oscillation mode at 0.5% constant strain over a frequency range of 0.05 and 50Hz at 6points/decade. The storage modulus (G'), a measure of the elastic energy stored during the deformation imposed by one oscillation of the rheometer, calculated by the Rheoplus software, was used as a measure of clot rigidity. The loss modulus (G"), the energy dissipated by the clot during deformation, was also recorded. Each condition was tested with at least 3 samples.

Rheology of fibrin and fibrin+ microgel matrices anticipates an alteration in the relaxation time of the system. For the fibrin +2mg/mL microgel condition, the relaxation time is expected to occur at lower frequencies or equivalently at longer times than the fibrin alone condition. This anticipated cross-over between G' and G'' at lower frequencies indicates that the fibrin-microgel matrix takes a longer time to relax or behave as a liquid. For a cell interacting in this system, longer relaxation times indicate that a cell would treat the fibrin-microgel matrix as an elastic component. However, because the data is for a bulk gel and not for more localized regions within the matrix, it is possible that the microgel colloidal assembly behaves as a viscous liquid component inside an elastic fibrin-fiber network.

With the addition of microgels into the clot structure, the storage modulus and loss modulus increase by approximately a factor of 3. Typically, when comparing the differences in mechanical strength for different materials, an order of magnitude change indicates a significant difference in properties. While the bulk difference for fibrin and fibrin+microgel networks is not over an order of magnitude, a factor of 3 difference in the shear strength could still possibly indicate significantly differences for a cell responding to these networks because of the shorter length scale interactions a cell has with its micro-environment.

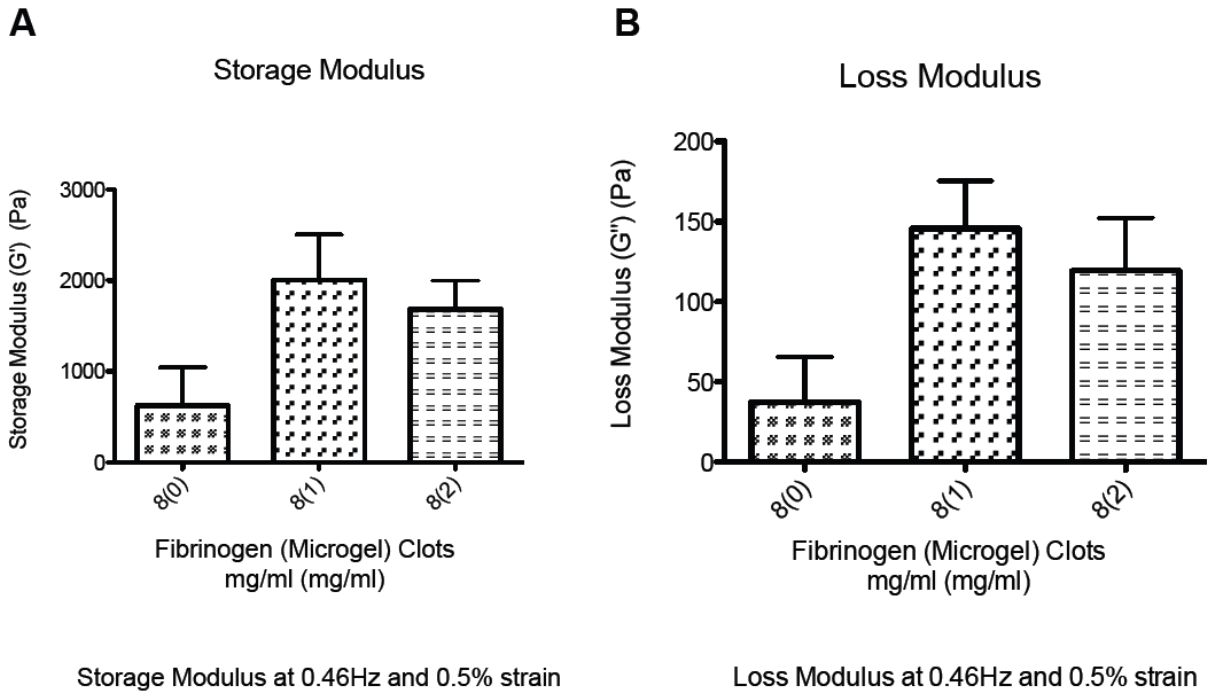

Figure 14. Storage and Loss Modulus of Fibrin-Microgel Gels. (A) Storage modulus of fibrin-microgel gels at 0.5% strain and 0.46Hz (B) Loss modulus of fibrin-microgel gels at 0.5% strain and 0.46Hz

Fibrin-Microgel Clot Bulk Compression:

In the clinical setting, fibrin concentrations in the physiological range that allow for acceptable cell growth and matrix remodeling are very difficult to handle. In order to enhance handleability, high protein concentrations are used to yield more rigid gels, but the ability of cells to grow in and remodel these matrices is hindered. By incorporating a colloidal microgel assembly into a fibrin matrix, the goal was to enhance the mechanical strength and handleability of a fibrin matrix but at lower protein concentrations that would allow for improved angiogenic properties. The young's modulus of fibrin-microgel gels was measured by uniaxial compression.

A Bose EnduraTEC™ ELF 3200 Uniaxial Testing System (Bose Corporation ElectroForce, Eden Prairie, MN) was used to perform compression tests on 4 and 8mg/mL fibrin clots containing 1 and 2mg/mL microgels. Clots were polymerized with 1U/mL thrombin in HEPES +Ca buffer for 2 hours in a silicone mold prior to taking measurements. The silicone mold consisted of two layers of a CoverWell™ perfusion chamber gasket (Invitrogen, Frederick, Maryland), 9mm in diameter and 2.5mm deep, with the final dimensions of the samples being

9mm in diameter and 5mm in height. Strain at 10, 20, 30, 40, and 50% were applied at 1Hz and all experiments were conducted at room temperature, with each condition being tested with at least 3 samples. The young's modulus at 20% strain was calculated and recorded for each condition.

Observing the young's modulus calculated for 20% strain, the microgels appear to increase the mechanical strength of a fibrin clot. These preliminary results show that for higher protein concentrations and higher microgel concentrations, the effect is multiplied. A larger sample size needs to be used to effectively determine any differences between groups, but the trend suggests that these space filling microgels occupy the free volume between fibers and provide added compressive strength to a fibrin network.

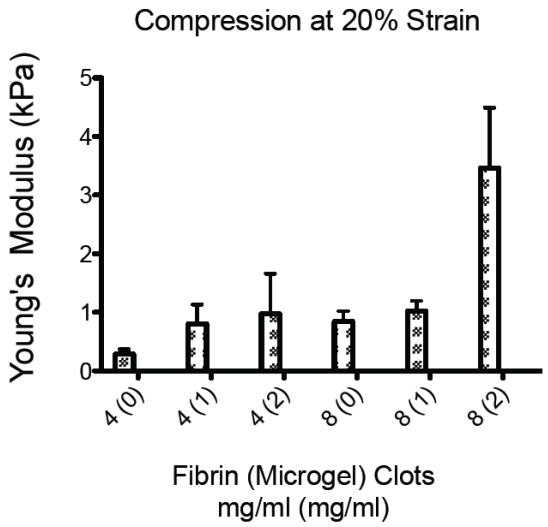

Figure 15. Young's Modulus of Fibrin-Microgel Gels Under Compression at 20% Strain

In order to better understand how cells will behave in these matrices, fibroblasts were incorporated into the hybrid fibrin-microgel polymerization reactions to monitor morphology and viability. It is necessary to analyze how these materials will affect cell fate and phenotype to allow for modifications in design criteria to the matrices.

NIH3T3 fibroblasts were cultured in 10% bovine calf serum with 1% penicillin/ streptomycin in Dulbecco's modified eagle medium with 2mM L-glutamine. For formation of the gels, polymerization reactions (100ul) consisted of 2mg/mL fibrinogen with 20% (v/v) cells and 1U/mL thrombin. Rubber gaskets were employed to allow for proper formation of the gels onto glass bottom dishes. Cells were prepared at a concentration of 750,000 cells per mL for 15,000 cells per sample. AFA (4-acrylamidofluorescein) microgels were added to the reaction for a final concentration of 1mg/mL (10ul of 10mg/mL stock). Either additional media was added as buffer or 25mM HEPES 150mM NaCl 1mM $CaCl_2$. Alexa Fluor 647 labeled fibrinogen was incorporated into the 2mg/mL final concentration at 10% of the total fibrinogen for visualization with confocal laser scanning microscopy.

Reactions were incubated at 37°C for two hours to allow for sufficient polymerization before an equal volume of media was added. The cells were then allowed to spread for an additional hour. After three hours total, the constructs were rinsed with Dulbecco's phosphate

buffered saline (1X PBS) with calcium and magnesium. The samples were then fixed for ten minutes in 4% formaldehyde at room temperature and then rinsed two times with 1X PBS. They were next permeabilized in 0.2% Triton X-100 for ten minutes. For visualization of the cell cytoskeleton, specifically filamentous actin, the samples were stained with Alexa Fluor 546 phalloidin (1:40 in 1X PBS) at room temperature for 1 hour. Hoechst 33258 was added for five minutes at 1:1000 for visualization of cell nuclei. Following staining, the samples were rinsed three times for five minutes with 1X PBS prior to imaging. Samples were imaged on a Zeiss 710 Laser Scanning Confocal Microscope using both the 20X and 63X objectives.

Below are confocal microscopic images of NIH3T3 fibroblasts in fibrin networks with and without 1mg/mL AFA microgels. Images were taken with a pinhole size of 1 airy unit and sections ranged from 20-80um in z-position with a 0.5um step size. We have demonstrated that cells can be kept viable within these constructs and subsequently fixed and stained for analysis.

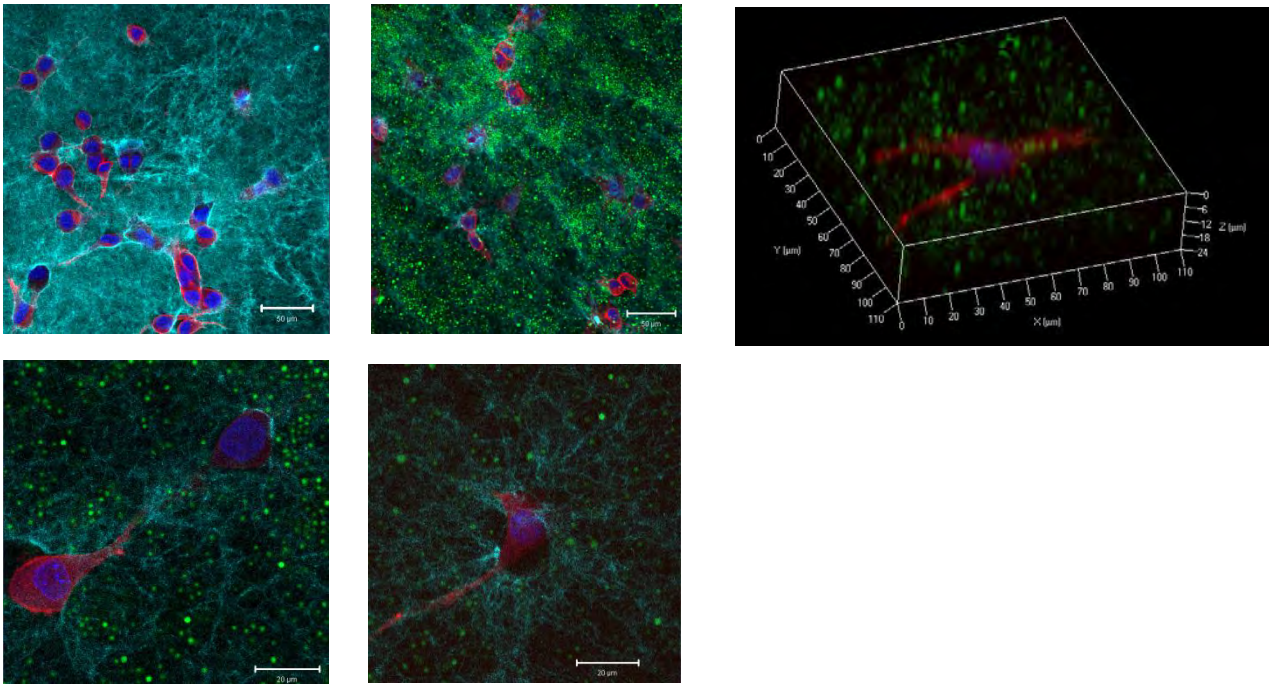

Figure 16: NIH3T3 fibroblasts in 3D hybrid matrices are viable and spread. Confocal images were taken with 20X objective (A,B) and 63X objective (C,D). A) Fibrin only control displaying spread morphology in the dense fibrin network. B,C,D,E) 2mg/mL fibrin with 1mg/mL AFA microgels show viable spread cells with space filling colloidal microgels at a high density. Panel E shows spatial scales of maximum intensity 3D projection with fibrin removed for better visualization. Microgels appear blurred in some areas as they are free flowing and have fluctuations in space throughout the scan. (Scale bars 50um (A,B) and 20um (C,D)).

In order to better observe the free flowing nature of the microgels, a time series video was taken of 0.25mg/mL AFA microgels within a 1mg/mL fibrin matrix and captured at 1 second per image for 10 seconds. The video shows 3 frames per second, capturing the diffusion of microgels within a fibrin network.

We are currently in the process of quantifying cell morphology and phenotype at various concentrations of fibrinogen and microgels. Protein conjugated microgels, including fibrin knob-peptides, will also be used to modify the matrix properties. We will also conduct longer term culture experiments to ensure the viability of the cells as they infiltrate and modify the matrix.

We aim to modulate the parameters of material synthesis in order to influence cell morphology and phenotype. Upon determination of the specific material characteristics, we will induce the differentiation of mesenchymal stem cells within these constructs.

Task 6: Determine the appropriate conditions for large-scale culture, decellularization, and lyophilization, of stem cell embryoid body (EB) extracellular matrices (ECM).

Mouse embryonic stem cells (ESCs; D3 cell line) were initially expanded on a feeder layer of mouse embryonic fibroblasts and were subsequently cultured feeder-free for several passages on 0.1% gelatin-coated 150 mm polystyrene cell culture dishes (Corning) with Dulbecco's modified eagle medium (Mediatech), supplemented with 15% fetal bovine serum (HyClone), 2 mM L-glutamine (Mediatech), 1x MEM non-essential amino acid solution (Mediatech), antibiotic/antimycotics (Mediatech), and 0.1 mM β- mercaptoethanol (MP Biomedicals, LLC). Undifferentiated cells were expanded prior to EB formation in the presence of 10^3 U/mL leukemia inhibitory factor (LIF) (ESGRO), which was added to the culture media upon each re-feeding. Cells were passaged every two to three days before reaching ~70% confluence. To initiate EB culture, ESCs were trypsinzed from the gelatin-coated dishes using 0.05% Trypsin/0.53 mM EDTA (Mediatech) and introduced into AggreWell™ 400 templates (Stem Cell Technologies) at a density of $6x10^6$ cells in 3 mL differentiation media (ESC media without LIF) to form 1000 cell EBs (~ 6000 microwells). After allowing the cells to initially settle in the insert wells, the multi-well plates were centrifuged for 5 minutes at 200xg. After 24 hours of culture, EBs were transferred from the AggreWell™ to rotary suspension culture with ~2000 EBs cultured in 100 mm bacteriological grade polystyrene Petri dishes (Corning) with 10 mL of differentiation media. EB suspension cultures were maintained on rotary orbital shakers (Barnstead Lab-Line, Model 2314) at 40 rpm at 37°C in 5% CO_2 for the entire duration of suspension culture. Previous work from our lab has demonstrated that rotary orbital suspension culture methods result in greater yields of homogeneous populations of EBs while preventing agglomeration of the 3D cell aggregates.

EBs were cultured in suspension for up to 12 days and re-fed every other day after collecting independent EB cultures via gravity-induced sedimentation in 15 mL conical tubes. Two different culture conditions were compared – serum-containing EB differentiation media (+serum) versus serum-free ESGRO media. The components of serum-containing media included Dulbecco's modified eagle medium, supplemented with 15% fetal bovine serum, 2 mM L-glutamine, 1x MEM non-essential amino acid solution, antibiotic/antimycotics, and 0.1 mM β-mercaptoethanol. The serum-free media used was ESGRO Complete media (Millipore). Spent media was aspirated, and the cultures were replenished with 10 mL of fresh differentiation media before being placed back in the Petri dishes and returned onto the rotary orbital shakers.

RNA was extracted from undifferentiated ESCs (day 0) and from EBs cultured in both +serum and ESGRO media on days 6, 9, and 12 of rotary culture utilizing the RNeasy Mini Kit (Qiagen) and analyzed on the NanoDrop spectrophotometer (NanoDrop) for concentration and purity at 260 nm and 280 nm. Complimentary DNA was reverse transcribed using 1 µg of total RNA in conjunction with the iScript cDNA synthesis kit (BioRad) on the iCycler Thermal Cycler (Bio-Rad). Quantitative RT-PCR was performed using SYBR Green with the MyIQ cycler (BioRad). Primer sets were designed using Beacon Designer software for housekeeping gene glyceraldehyde-3-phosphate dehydrogenase (Gapdh), as well as bone morphogenic protein-4 (Bmp-4), fibroblast growth factor-2 (Fgf2), insulin-like growth factor-2 (Igf2), and vascular endothelial growth factor-A (Vegfa).

During EB feedings at days 9 and 12, conditioned media from both +serum and ESGRO

cultures was collected. After 48 hours of conditioning, EBs were collected by gravity-induced sedimentation and the EB-CM (~10 mL) was transferred to a fresh conical tube. The spent media was centrifuged for 5 minutes at 10,000 RPM at 4°C to remove cellular debris and the supernatant fraction was transferred to a new 15 mL conical tube and stored at -20°C prior to further analysis.

Proteins were extracted from lyophilized EB matrices (EBM) from later days of differentiation (day 9 and day 12) using tissue protein extraction buffer (TPER, Thermo). TPER buffer is mild enough that proteins can be assessed using immunoassays. For both TPER and serum-free media EBM extractions, each lyophilized EBM sample was obtained from a single plate of EBs (~2500 EBs) and extracted with 500 □L of TPER buffer with rotation for two hours at room temperature. Before EBM protein analysis was performed, all samples (n=6 per group) were centrifuged to remove insoluble matrix for 5 minutes at 14,000 RPM at room temperature. Specific growth factors, including BMP-4, IGF-2, FGF-2, and VEGF-A, extracted from the EBM were quantified using enzyme-linked immunosorbent assays (ELISAs) obtained from R&D Systems.

The gene expression of several growth factors known to be involved in muscle regeneration and angiogenesis were differentially expressed in EBs cultured in +serum compared to ESGRO media. Genes of growth factors involved in angiogenesis, including Bmp4, Fgf2, and Vegfa, were expressed at similar levels if not higher, in EBs cultured in ESGRO compared to +serum. Igf2, a growth factor known to stimulate muscle regeneration, was expressed at similar levels at earlier days of differentiation (days 6 and 9) but was increased by day 12 in +serum EBs.

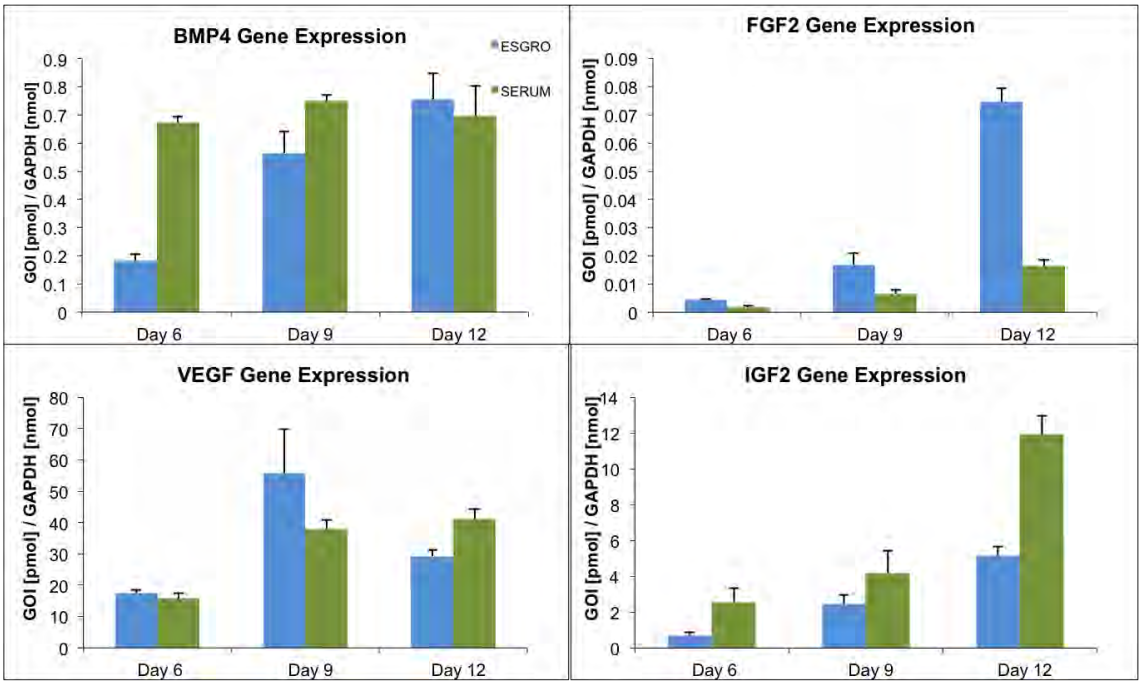

Figure 1. Growth factor gene expression comparison between ESGRO- and +serum-cultured embryoid bodies during differentiation time. Sample size n = 6, mean ±

Growth factor proteins generated by EBs during differentiation were quantified in the matrix associated fraction (EB matrix) over differentiation time. Following protein extraction from EBM with TPER buffer, the same four growth factors previously analyzed for gene expression and soluble protein content were examined. At both 9 and 12 days, the amount of BMP4 and FGF2 extracted from ESGRO EBM and +serum EBM was similar between the treatment groups. However, the differences in specific protein content were evident in the VEGFA and IGF2 proteins. The ESGRO EBM exhibited higher levels of VEGFA in the TPER extraction compared to +serum EBM. On the other hand, IGF2 content was higher in +serum EBM extraction compared to ESGRO EBM extractions, which appeared to increase at day 12 compared to day 9.

Overall, the culture conditions exhibited differences in the growth factor gene expression and in turn resulted in the differential protein expression secreted by the EBs as well as the protein associated with the matrix. These differences will aid in determining the conditions in which EBs will be cultured to further the development of 3D scaffolds to aid in composite tissue repair.

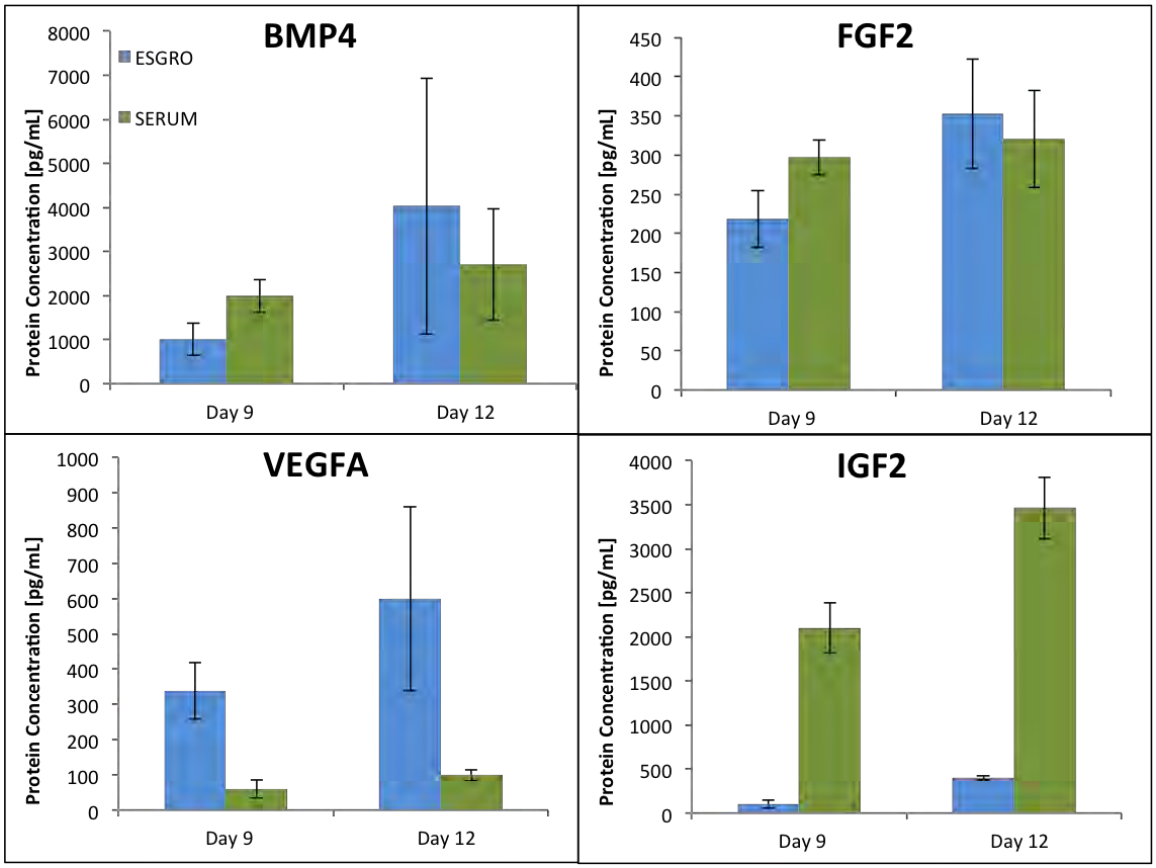

Figure 2. Matrix-associated growth factor protein comparison between ESGRO- and +serum EB matrices during differentiation time. Sample size n = 6, mean ± standard deviation.

In order to obtain a more global view of the growth profile differences between the two EB culture conditions, SuperArray analysis will be performed over samples collected during differentiation. This array analysis will further aid in assessing which growth factors are being differentially expressed, particularly ones that stimulate tissue repair, and ultimately determining

the treatment condition and time point at which stem cell matrix should be utilized for 3D scaffold implementation.

Specific Aim 4. Adapt percutaneous stem cell delivery strategies for craniofacial cartilage defect repair.

Task 1. Characterize rat ear and nasal chondrocytes with respect to extracellular matrix production at the mRNA and protein levels and as a function of passage number.

Task 2. Characterize human auricular and nasal chondrocytes with respect to extracellular matrix production at the mRNA and protein levels and as a function of passage number.

Human auricular chondrocytes were isolated from children undergoing otoplasty at Children's Healthcare of Atlanta. Isolated cells were expanded in culture and phenotype examined at each passage. Confluent cultures were treated with doses of 1α,25(OH)2D3 or 24(R),25(OH)2D3 and protein kinase c measured after 9 minutes and alkaline phosphatase specific activity measured after 24 hours. RNA was harvested from confluent cultures and mRNA levels of chondrogenic markers SOX9, COL2, COMP, and ACAN measured by real-time PCR.

Cells increased PKC (Fig. 17) and alkaline phosphatase specific activity (Fig. 18) in response to 1α,25(OH)2D3 and 24(R),25(OH)2D3 in a dose-dependent manner. However, magnitude of the response diminished as cells were passaged. Levels of mRNA for markers of chondrocyte phenotype SOX9, COL2, COMP, and ACAN also decreased as passage number increased (Fig. 19).

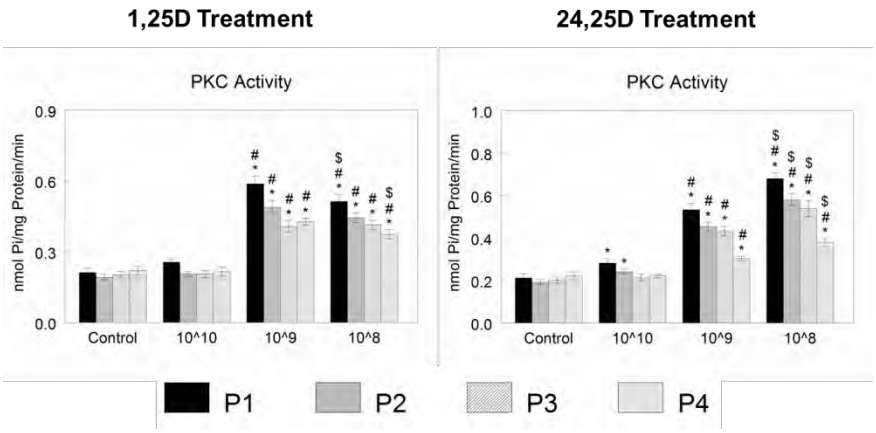

Fig. 17. Response of human auricular chondrocytes to 1α,25(OH)2D3 and 24(R),25(OH)2D3. Cultures were treated with 1α,25(OH)2D3 or 24(R),25(OH)2D3 at passage 1 (P1), 2 (P2), 3 (P3), or 4 (P4) for 9 minutes and PKC activity measured. *p<0.05, vs. control; #p<0.05, vs. 10^{-10}M; $p<0.05, vs. 10^{-9}M.

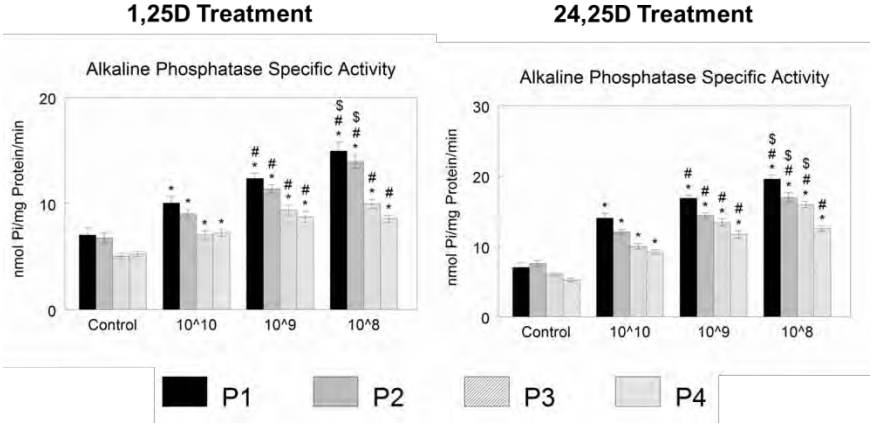

Fig. 18. Response of human auricular chondrocytes to 1α,25(OH)2D3 and 24(R),25(OH)2D3. Cultures were treated with 1α,25(OH)2D3 or 24(R),25(OH)2D3 at passage 1 (P1), 2 (P2), 3 (P3), or 4 (P4) and alkaline

phosphatase specific activity measured after 24 hours. *p<0.05, vs. control; #p<0.05, vs. 10^{-10}M; $p<0.05, vs. 10^{-9}M.

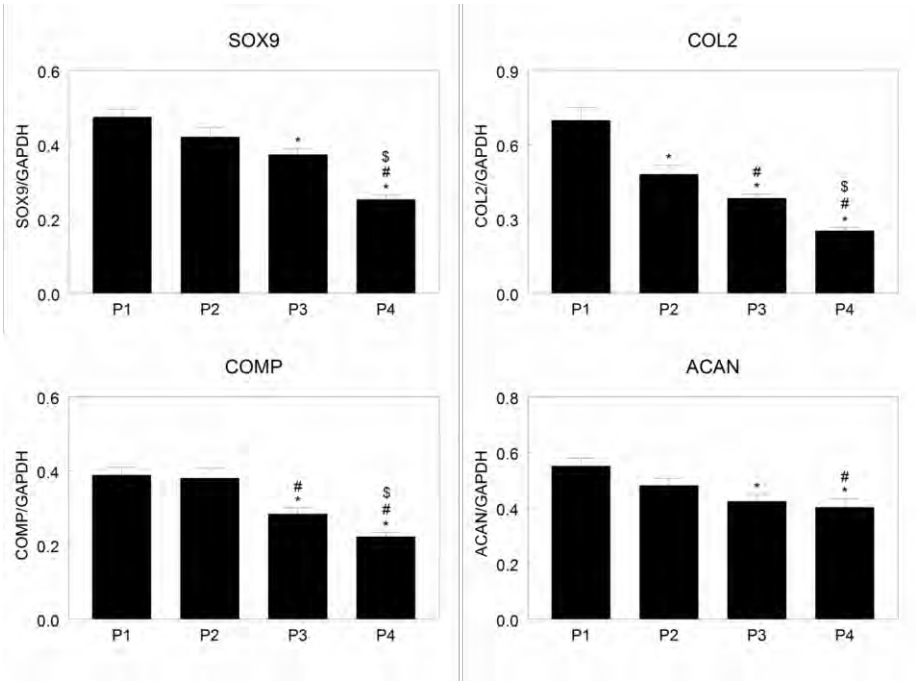

Fig. 19. Chondrogenic phenotype of human auricular chondrocytes. Cultures were harvested after passage 1 (P1), 2 (P2), 3 (P3), or 4 (P4) and mRNA levels of chondrogenic markers SOX9, COL2, COMP, and ACAN measured by real-time PCR. *p<0.05, vs. control; #p<0.05, vs. 10^{-10}M; $p<0.05, vs. 10^{-9}M.

Task 3. Optimize protocol for inducing rat ASCs to express a hyaline cartilage phenotype.

Fat was isolated from the abdomen and breast of six female donors aged 18 to 49 under an IRB approved protocol at the Georgia Institute of Technology. ASCs were isolated using a digestion cocktail of collagenase 1A, dispase, and trypsin. Cells were then plated at 5,000 cells/cm^2 in Lonza Mesencyhmal Stem Cell Growth Medium (MSCGM) until they reached 90% confluence. They were then either replated or microencapsulated (uB) at 10x10^{6}cells/cm^3 in 20mg/ml LVM alginate through a 28G needle at 6.0kV/cm. Plated and microencapsulated ASCs were then treated for 7 or 14 days with MSCGM or chondrogenic media (CM) containing 10 ng/ml TGF-β1 and 100 ng/ml BMP-6. RNA was extracted at day 7 and at day 14 of culture and converted to cDNA for quantitative real time PCR. The genes quantified and normalized to the housekeeping gene Rps18 were colII, aggrecan, sox-9, tgfb1, tgfb2, tgfb3, nog, colX, comp, fgf2, pthlh, igf1, and vegfa. Media was collected on days 8 and 15 and quantified using R&D system ELISA kits. FGF2, IGF-I, Tgf-ß3, and VEGF-A were measured and normalized to DNA content were. Results were analyzed using a multi-way ANOVA test.

Microencapsulated ASCs showed increased production of IGF-I, FGF2, and TGF-ß3 as compared to monolayer ASCs. Production of TGF-ß3 was greatest when the ASCs were not only microencapsulated but also when they were treated with CM. Both monolayer and microencapsulated ASCs had significantly decreased production of VEGF-A when CM added, compared to those cells cultured with MSCGM. Furthermore, significant amounts of VEGF-A and FGF2 were trapped within the alginate microbeads. ANOVA analysis showed that the interaction of media and microencapsulation had a significant effect on growth factor expression

and production. Additionally, ANOVA confirmed that the donors themselves had no significant effect on growth factor expression or production. ***Chondrocyte Phenotype*:** ASCs treated with CM had increased expression of Acan and Comp compared to ASCs treated with MSCGM. ColX expression was increased in both microencapsulated and monolayer ASCs treated with CM. Noggin, the BMP inhibitor, showed highly increased expression in the monolayer ASCs treated with CM, but this effect was diminished when the cells were microencapsulated. ***Chondrocyte proliferation:*** Igf1 expression showed a significant increase over microencapsulated ASCs when CM was added. Pthlh had the greatest expression in the microencapsulated cells treated with MSCGM. Tgfb1 had the greatest expression in microencapsulated ASCs treated with CM and Tgfb2 had a similar increase in expression with microencapsulated ASCs treated with both MSCGM and CM. ***Angiogenic factors:*** Microencapsulated and plated ASCs showed decreased expression of both Fgf2 and VegfA as compared to those cells treated with MSCGM.

Task 4. Apply for ACURO approval for the rat xyphoid and rabbit implantation models.

Protocol 08346012.04 entitled, "Creation of a Rat Model of Cartilage Defect: A Template for Human Chondrocytes," IACUC Protocol Number A09041, Principal Investigator Barbara Boyan, was approved for the use of rats. This protocol was approved on April 15, 2010 for our FY2008 funding. We will be working with this protocol until the FY2008 funding period ends on 9/29/2011. At that time we will transfer the protocol to the new FY2010 appropriation funding. Please see approval on Appendix # 2.

Task 5. Apply for IRB/HRPO approval for use of human ear and nose cartilage cells.

We have IRB approval from Georgia Tech's IRB committee for use of human ear and nose cartilage. We submitted an HRPO application and received approval on July 19, 2011. Approval e-mail is attached.

Task 6. Perform rat xyphoid defect study for microencapsulated rat ASCs and prechondrocytes.

We have completed the *in vivo* study investigating the effect combing a RGD-hydrogel scaffold with ASC microbeads has on cartilage regeneration using the xiphoid defect animal model. Below are the description of the experiment and the results.

P1 ASCs isolated from male Sprague Dawley were microencapsulated (uE) at $25x10^6$cells/cm^3 in 20mg/ml LVM alginate through a 28G needle at 6.0kV/cm and treated with growth medium or chondrogenic medium (CM) for 5 days. Prior to surgeries, sterile RGD-conjugated alginate (NOVATACH M RGD, FMC BioPolymer) was dissolved in DMEM containing 1% penicillin and streptomyocin at a concentration of 25 mg/mL and mixed with sterile 20 mg/mL $CaSO_4$ (Sigma) at a 4:1 volume ratio using two syringes connected to a luer-lock 3-way connector. During surgeries, 2 mm cylindrical defects were made in the xiphoids of 120g male Sprague-Dawley rats. ASC microbeads were implanted into the defect, immobilized with the RGD-conjugated hydrogel mixture, and covered with SEPRAFILM®. Empty defects with the hydrogel mixture and re-implanted excised cartilage (autografts) served as controls in the 2 mm study. All groups were tested in 7 rats. After 35 days, xiphoids were explanted, x-rayed, and incubated in a 40% Hexabrix solution for equilibrium partitioning of an ionic contrast agent-microcomputed tomography (EPIC-μCT) to visualize and quantify proteoglycan distribution. Samples were then fixed in 10% phosphate-buffered formalin (Sigma) for 48 hours and embedded in paraffin. Sagittal sections of the defect were stained with safranin-O using a

fast green counter stain to evaluate proteoglycan present. Statistical differences among these experimental groups were determined via ANOVA with a post hoc Tukey test (GraphPad Prism). All differences and effects were considered to be statistically significant if the p-value was less than 0.05.

X-ray scoring of defects showed that defects with GM or CM preconditioned ASC microbeads and hydrogel mixture performed better than empty defects with only the hydrogel. Defects with only the hydrogel mixture had no apparent cell infiltration, new extracellular matrix (ECM) deposition, or perichondrium as indicated by the lack of fast green staining (Figure 20). Defects with the ASC microbeads preconditioned in MSCGM had traces of fast green staining throughout the defect with cell infiltration and tissue deposition at the edges of the defect (Figure 20). Defects with ASC microbeads preconditioned in CM had ECM deposition throughout the defect with cell infiltration, tissue resembling a perichondrium, and initial proteoglycan deposition (Figure 20). Defects with the autograft had cell infiltration, a perichondrium that resembled that of the surrounding xiphoid and proteoglycan deposition between the edges of the defect and autograft (Figure 20). EPIC-μCT measured cartilage volume was highest for the autograft group, and no difference in cartilage volume was seen in any defect containing the hydrogel mixture (Figure 20).

Subsequent investigation revealed that a noticeable amount of hexabrix was retained within alginate constructs after incubation overnight. This finding was highly surprising because of alginate polymer's negative charge and because of the ability of alginate microbeads to provide extended release of high pI proteins. However, it may be possible that the negatively charged hexabrix may have interacted with the calcium crosslinks in alginate gels. Because the ability of EPIC-μCT to visualize and quantify proteoglycan production is dependent on hexabrix exclusion from the anionic tissue, this method may not be optimal for detecting neocartilage formation within alginate constructs.

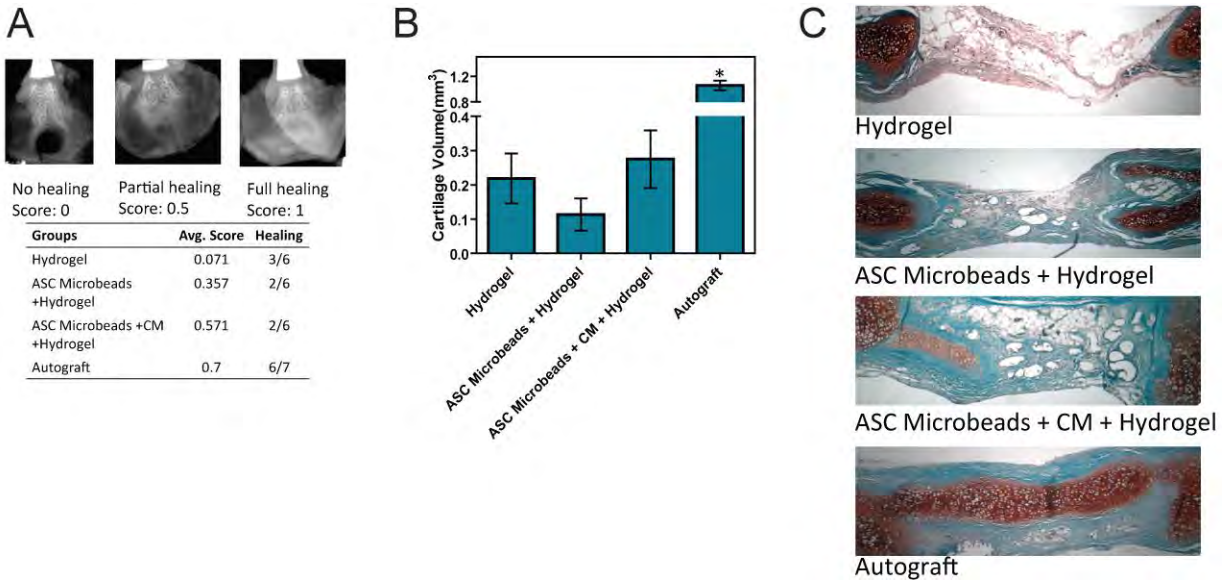

Groups	Avg. Score	Healing
Hydrogel	0.071	3/6
ASC Microbeads +Hydrogel	0.357	2/6
ASC Microbeads +CM +Hydrogel	0.571	2/6
Autograft	0.7	6/7

Figure 20: ASC Microbeads and RGD-Hydrogel Mixture in Xiphoid Defect
(A) Radiographic scoring. (B) 3-D EPIC-μCT calculated cartilage volume within defects (n=7±SE, *p<0.05 vs. all groups). (C) Representative Safranin-O staining of 2 mm defects.

Task 7. Complete optimization protocols for rat and human ASCs and induced chondrocytes (prechondrocytes) by assessing the viability and phenotype of ASCs and prechondrocytes loaded on silk nanofiber meshes.

Silk/fibroin 3D porous scaffolds were prepared from silk fibroin solution using salt-leaching techniques as described in the literature [1]. Briefly, 7% (W/V) silk fibroin water solution was extracted from degummed biombyx mori ployhybrid silkworm cocoon. 4 g of granular NaCl (particle size 300-500 μm) was added to 2 mL silk fibroin solution in 35mm petri dish to allow gelation at room temperature for 2 days. The formed sponges were then washed against distilled water for 3 days to remove the salt and dried in air. Before cell seeding, the sponges were rehydrated in distilled water for 2 hours and formed into cylinders (6mm in diameter and 3mm in thickness) using a biopsy punch (Miltex, London, UK). Scaffolds in aqueous suspension were autoclaved at 121°C for 15 min. After cooling to room temperature, the water was removed and incubated overnight with culture media at 37°C, 5% CO_2. After conditioning the scaffolds, the bubbles inside of the scaffolds were removed by syringe-vacuum system as described previously. The scaffolds were ready for cell seeding after blot dry.

Adipose stem cells were isolated from inguinal fat pads of the hind legs of Sprague Dawley rats with serial enzymatically digestions as described in the literature [2]. Briefly, the adipose tissue was pooled and digested in 0.25% trypsin for 30 minutes. The tissue was then cut into small pieces and then digested in 9125 units of collagenase IA (Sigma, St. Louis, MO) and 75 units of dispase (Gibco, Invitrogen, Carlsbad, CA) IA for 4 hours. The upper layer of adipocytes was removed, and the cell suspension was filtered through a 40 μm cell strainer and then was collected by centrifugation. ASCs were plated at 5,000 cells/cm2 and cultured in T175 flasks with commercially available stem cell growth media (GM) (Lonza, Basel, Switzerland) containing 10% FBS, 1% penicillin-streptomycin in a humidified, 95% air/5%CO_2 atmosphere at 37°C. Primary passage confluent cells were used for seeding on scaffolds.

Each scaffold was placed in the center of each well of a 12-well plate containing 200μL of growth media. To seed the scaffolds, 1 x 10^6 P1 ASCs were loaded on the top of the scaffolds through pipette tips. 4 hours after cells seeding, 1.5 mL of growth media was added to each well. 6 hours after cell seeding, samples either remained in a static culture or were subjected to a rotation culture at 50 rpm on an orbital rocker. After 72 hour of culture, the ASCs/silk scaffolds were then transferred to new plates and the media was replaced with either the same growth media as the initial culture or replaced with commercially available chondrogenic media (CM) (Lonza, Basel, Switzerland). Four experimental groups of scaffolds were obtained: growth media + static culture (GMS), growth media + rotation culture (GMR), chondrogenic media + static culture (CMS), and chondrogenic media + rotation culture (CMR). The ASCs/silk scaffolds were maintained in a humidified, 95% air/5% CO_2 atmosphere at 37°C. The media was changed every two days for up to 28 days of culture.

In order to determine the appropriate time for cells to attach on the scaffolds, seeded scaffolds were maintained under static culture for 6h, 12h, or 24h before rotation culture. At the end of each culture period, unincorporated cell numbers were measured using a Beckman Coulter Cell Counter (Beckman Coulter Inc., Miami, FL). Cell seeding efficiency was then calculated using the formula:

$$\text{Cell seeding efficiency (\%)} = \left(1 - \frac{\text{Unincorporated cell numbers}}{\text{Initial cell seeding numbers}}\right) \times 100\%$$

The viability of ASCs in the scaffolds was examined by a Live/Dead® assay (Invitrogen Corporation, Carlsbad, CA, USA) as described in the literature [1]. Briefly, ASCs/silk scaffolds

were washed twice with PBS for 5 min, and then incubated with 2μM calcein AM and 4μM EthD-1 in PBS for 30 min at room temperature. After removing extra dyes by washing in PBS for 5 min, the scaffolds were sliced in half, and the images were taken from both the surface and the center of the scaffolds using Ziess LSM 510 VIS confocal microscopy (Carl Ziess Inc., Japan) with an excitation wavelength of 495nm and an emission wavelength of 515nm.

Cell Proliferation

Cell proliferation in scaffolds was evaluated at 1d, 7d, 14d, 21d, and 28d after the initial seeding using an alamarBlue® assay (AbD Serotec, Raleigh, NC, USA) according to the manufacturer's instructions. Briefly, seeded scaffolds were incubated with 1 mL of 10% alamarBlue® reagent in culture medium for 2h in humidified, 95% air/5% CO_2 atmosphere at 37°C. At the end of incubation, 100μL of the supernatant was then transferred to a 96-well plate and fluorescence intensity was determined with a micro-plate reader (Spectromax Gemini XS, Molecular Devices, Sunnyvale, CA, USA) (excitation/emission: 565nm/595nm). Media incubated with non-seeded scaffolds were used as controls, and their fluorescence value was subtracted from those of cell-seeded scaffolds.

ASCs/silk scaffolds were harvested at day 14 and day 28. Total RNA was isolated from the silk scaffolds using an RNeasy kit® (Qiagen Inc., Valencia, CA, USA) and was quantified using a NanoDrop spectrophotometer (Thermo Scientific, Waltham, MA, USA). 1μg of total RNA was reverse-transcribed into cDNA using a High Capacity Reverse Transcription cDNA kit (Applied Biosystems, Carlsbad, CA, USA) according to the manufacturer's instructions. Realtime quantitative PCR were performed to measure the expression of cartilage related genes including sox9, col 2a1, acan, comp, col 1a1 and col 10a1 and normalized to RPS18. The amplification of genes was carried out on a StepOnePlus Real-time PCR System using Fast SYBR® Green Master Mix (Applied Biosystems, Carlsbad, CA, USA) with specific primers as list in supplemental table 1.

Beginning of rotation culture after 6h, 12h, and 24h of cell seeding resulted in a cell seeding density of 89.7%±1.5%, 91.2%±1.2%, and 91.3%±5.3%, respectively. No significant differences were found among the three different time points (P>0.05). Therefore, 6h after seeding was chosen for subsequent experiments in order to achieve potentially more homogenous cell distribution.

The live/dead assay revealed few detectable dead cells while the majority of cells were alive as stained green (Fig.21). Additionally, the distribution of cells throughout the scaffold was similar among all the groups. Cells in each groups distributed on and in the spaces between the red stained silk scaffolds. Majority of cells located close to the surface of the scaffolds with fewer cells found in the center of the scaffolds.

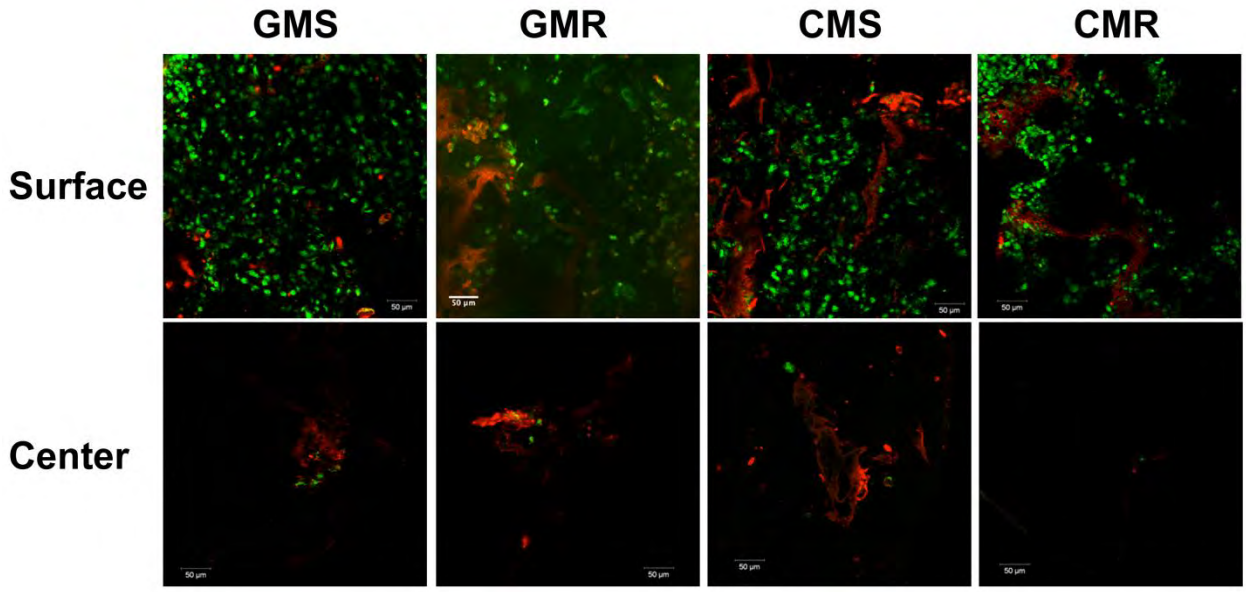

Figure 21. Cell viability analysis of ASCs/silk scaffolds under different culture conditions. ASCs/silk scaffolds after 28 days of culture under various conditions were stained with a Live-Dead® kit and then observed with confocal microscopy. A: scaffolds cultured in growth medium under static condition; B: scaffolds cultured in growth medium under rotation condition; C: scaffolds cultured in chondrogenic medium under static condition; D: scaffolds cultured in chondrogenic medium under rotation condition. Green staining represents live cells while red staining represents dead cells and stained silk scaffolds. Scale bar = 50 μm.

The amount of metabolite of alamar blue is in proportion to the cell number. Therefore, alamar blue assay was employed to monitor the change of cell numbers during 28 days of culture. As shown in Fig. 22, at day 1, there no significant difference among the groups. While the cell number of ASCs in all groups increased over the course of culture, ASCs/silk scaffolds cultured in growth medium under rotation culture exhibited the statistically significant greatest increase in cell number among all the groups (P<0.05). Moreover, the increase in cell number reached the platform between day21 and day28. Interestingly, ASCs/silk scaffold cultured in chondrogenic medium exhibited a slight decrease in cell proliferation between day 7 and day 14, but resumed the increase trend in the following weeks.

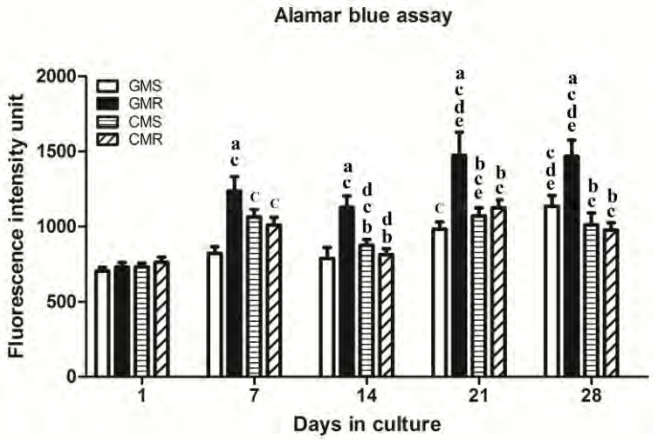

Figure 22. Cell proliferation of ASCs/silk scaffolds under different culture conditions. Alamar blue assay was used to monitor the cell proliferation over the course of culture. White bar represents scaffolds cultured in growth medium under static condition (GMS); black bar represents scaffolds cultured in growth medium under rotation condition (GMR); striped bar represents scaffolds cultured in chondrogenic medium under static condition (CMS), and slashed bar represents scaffolds cultured in chondrogenic medium under rotation condition (CMR). Each bar represents

the mean and standard error of *n*=6 independent cultures. [a]*P*<0.05 vs. GMS group; [b]*P*<0.05 vs. GMR group; [c]*P*<0.05 vs. Day1; [d]*P*<0.05 vs. Day7; [e]*P*<0.05 vs. Day14.

ASCs/ silk scaffolds cultured in chondrogenic medium elicited statistically significant higher gene expression of chondrogenic marker (sox9, col 2, acan and Comp) in comparison to those cultured in growth medium (Fig.23). In addition, static culture resulted in a relatively higher expression level of col2, aggrecan and comp at day 14 and day 28 respectively, while the expression of sox9 at day 28 is higher in the CMR group than CMS group. Furthermore, the expression of acan and comp increased at day 28 compared to day 14. However, the grater expression of col1 was also induced by chondrogenic medium compared to growth medium. Moreover, ASCs cultured in chondrogenic medium under static condition expressed the highest expression level of hypertrophic gene col10 at day 14. However, no significant difference of col10 expression level between different culture medium was observed at day28, while its expression level was higher under rotation culture compared to static culture.

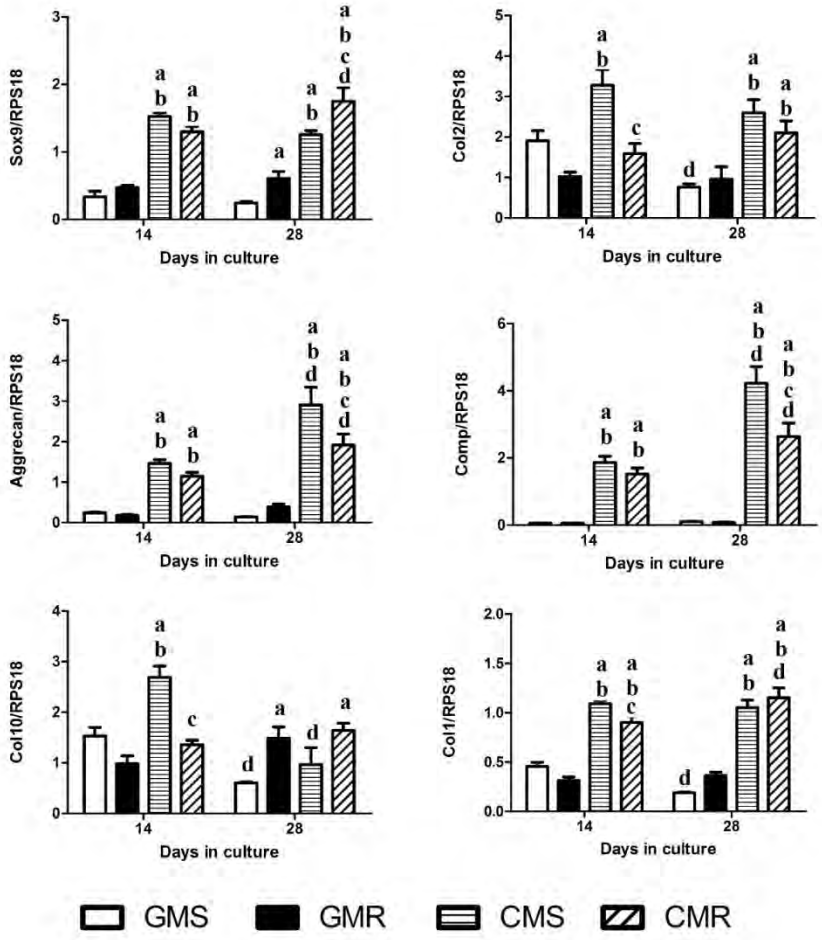

Figure 23. Real-time PCR analysis of cartilage-related gene expression in ASCs/silk scaffolds under different culture conditions for 14days or 28days. White bar represents scaffolds cultured in growth medium under static condition (GMS); black bar represents scaffolds cultured in growth medium under rotation condition (GMR); striped bar represents scaffolds cultured in chondrogenic medium under static condition (CMS), and slashed bar represents scaffolds cultured in chondrogenic medium under rotation condition (CMR). Each bar represents the mean and standard error of *n*=6 independent cultures. [a]*P*<0.05 vs. GMS group; [b]*P*<0.05 vs. GMR group; [c]*P*<0.05 vs. CMS group; [d]*P*<0.05 vs. Day14.

The production of GAG in the medium steadily increased along the culture time (Fig.24A). The amount of GAG found in the medium form CMS and CMR groups were more than 10 times higher than those cultured in growth medium at all time points tested. The similar pattern was also observed for GAG in the scaffolds. Chondrogenic medium induced 2 times of GAG production over growth medium (Fig.24B). Although a slightly lower amount of GAG in the medium was detected under rotation culture compared to static culture at some time points, significant lower GAG production after 28 days of culture in chondrogenic media under rotation was found at the scaffolds level.

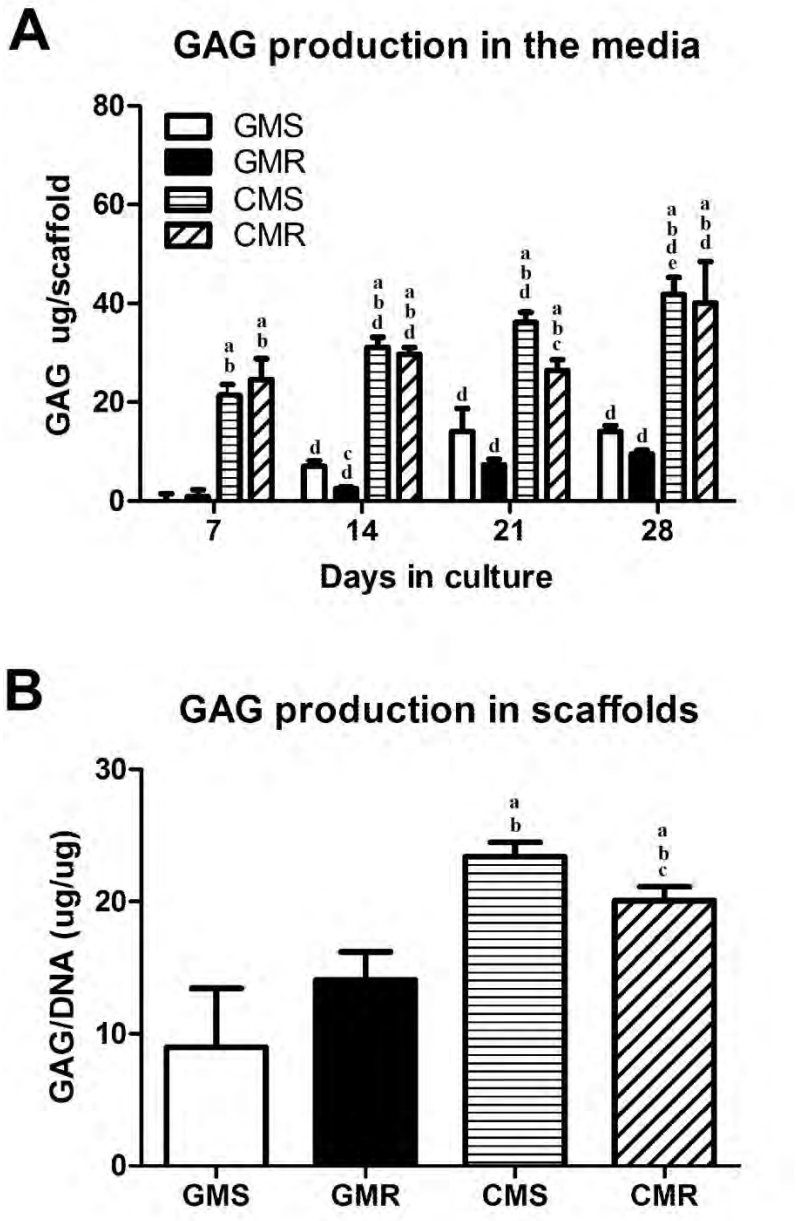

Figure 24. Glycosaminoglycan production and Young's modulus of different scaffolds. The amount of glycosaminoglycan (GAG) in both medium (A) and scaffolds (B) were measured using BMMB assay and normalized to DNA content of scaffolds. White bar represents scaffolds cultured in growth medium under static condition (GMS); black bar represents scaffolds cultured in growth medium under rotation condition (GMR); striped bar represents scaffolds cultured in

chondrogenic medium under static condition (CMS), and slashed bar represents scaffolds cultured in chondrogenic medium under rotation condition (CMR). Each bar represents the mean and standard error of n=6 independent cultures. [a]P<0.05 vs. GMS group; [b]P<0.05 vs. GMR group; [c]P<0.05 vs. CMS group; [d]P<0.05 vs. Day7 scaffolds, [e]P<0.05 vs. Day 14 scaffolds.

This result was also confirmed by safranin-O/fast green staining of scaffold sections (Fig. 25). While majority of cells the GMS, GMR, and CMR groups were stained green, cells in CMS groups displayed light red staining indicating the presence of GAG in the extracellular matrix. Immunofluorescence staining against collagen type II, Aggrecan and collagen type I protein also revealed the production of these proteins in ASCs/silk scaffolds under different culture conditions. Limited staining of collagen type II and Aggrecan were observed in ASCs/silk scaffolds cultured in growth medium, whereas abundant staining on the cells surface as well as in the extracellular matrix were found in those cultured in chondrogenic medium. Furthermore, static culture results in stronger staining than rotation culture in the same chondrogenic medium. No significant difference in terms of collagen type I production was observed among all the groups.

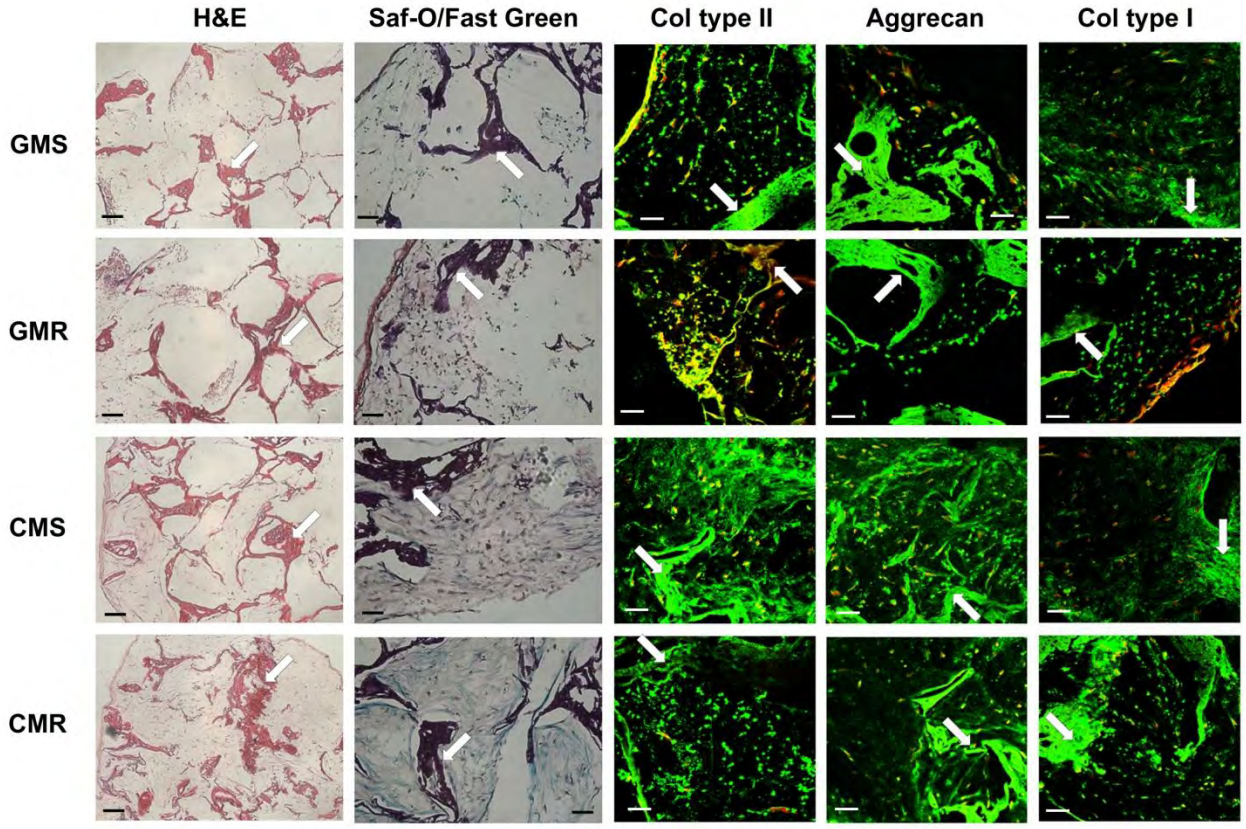

Figure 25. Histology analysis of ASCs/silk scaffolds under different culture conditions. Scaffolds were harvest after 28days of culture. After serial histological processing, scaffolds were sectioned into 8μm slices and subjected to H&E (Scale bar = 50 μm) and safranin O/fast green staining (Scale bar = 100 μm, red represents glycosaminoglycan) or immunofluorescence staining against collagen type II, Aggrecan and collagen type I protein with propidium iodide counterstaining of nuclei (Scale bar=100 μm green represents target proteins and red represents nuclei). White arrow indicates the silk scaffolds.

Specific Aim 5. Develop graft technologies for palate reconstruction.

Task 1. Obtain IACUC and ACURO approvals for a nude rat palate repair model.

Protocol 10188001.02 entitled, "Evaluation of Palate Graft Formulation to Enhance and Protect Implant Osseointegration," IACUC protocol number A10054, Principal Investigator Barbara Boyan, was approved for the use of rats. This protocol was approved on May 12, 2011. Please see Appendix # 3.

Task 2. Develop methods for decellularizing human palate tissue.

We are currently working with the Musculoskeletal Transplant Foundation (MTF) to develop methods for decellularizing human and rat palate tissue. We are still in the trial and error stage. The IACUC and ACURO for this project were approved during this year. The ACURO number is 10188001.04 for IACUC number A11080 and ACURO number 10188001.02 for A10054.

Task 3. Develop methods for loading decellularized human palate tissue with ASCs (without microbeads and with microbeads).

We are currently working with the Musculoskeletal Transplant Foundation (MTF) to develop methods for decellularizing human and rat palate tissue. We are still in the trial and error stage. The IACUC has been approved and the defect model is in planning stages.

Specific Aim 6. Adapt stem cell delivery technology for treatment of large bone defects.

Task 1. Obtain IACUC and ACURO approval for use of human stem cells on fiber mesh scaffolds in critical size defects in the rat.

The renewal of protocol 08346012.05 entitled, "Adipose-Derived Stem Cells for the Treatment of Long Bone Defects," IACUC protocol number A09048, Principal Investigator Barbara Boyan, was approved for the use of rats. This protocol was approved on November 3, 2010 under our FY2008 funding. We will be working with this protocol until the FY2008 funding period ends on 9/29/2011. At that time we will transfer the protocol to the new FY2010 appropriation funding. Please see approval on Appendix # 4.

Task 2. Obtain IRB/HRPO approval for obtaining human ASCs.

We had a meeting with Susan Kitchen from the HRPO Office on June 28, 2011 and we have now transferred our current HRPO approval A-15025a from our FY2008 grant to our FY2010 grant. The Protocol is entitled “Acquisition of Human Adipose Derived Mesenchymal Cells," for Proposal Log Number *OB346012,* Award Number WB1XWH-OB-1-0704, HRPO Log Number A-15025.a.

Task 3. Determine if human ASCs are viable in microbeads and assess their osteogenic differentiation potential and growth factor release.

Human ASCs were isolated from a 28 year old female donor. After passage 1, hASCs were microencapsulated (uE) into alginate microbeads at 10*10^6 cells/ml or passed and cultured on tissue culture polystyrene (TCPS). Cells were cultured one week in Lonza Mesenchymal Stem Cell Growth Media (GM) to allow the microencapsulated cells to adjust to their new environment within the alginate microbead. hASC cultures were cultured for 15 days with GM or cultured in osteogenic media (OM) to induce osteogenic differentiation. After two weeks, protein secretion was analyzed. Microencapsulation did not increase osteogenic factor production but increased

the angiogenic factors produced which play an important role in the bone healing process. The osteogenic potential of the hASCs was not enhanced by osteogenic media.

Similar experiments will be done with future donors.

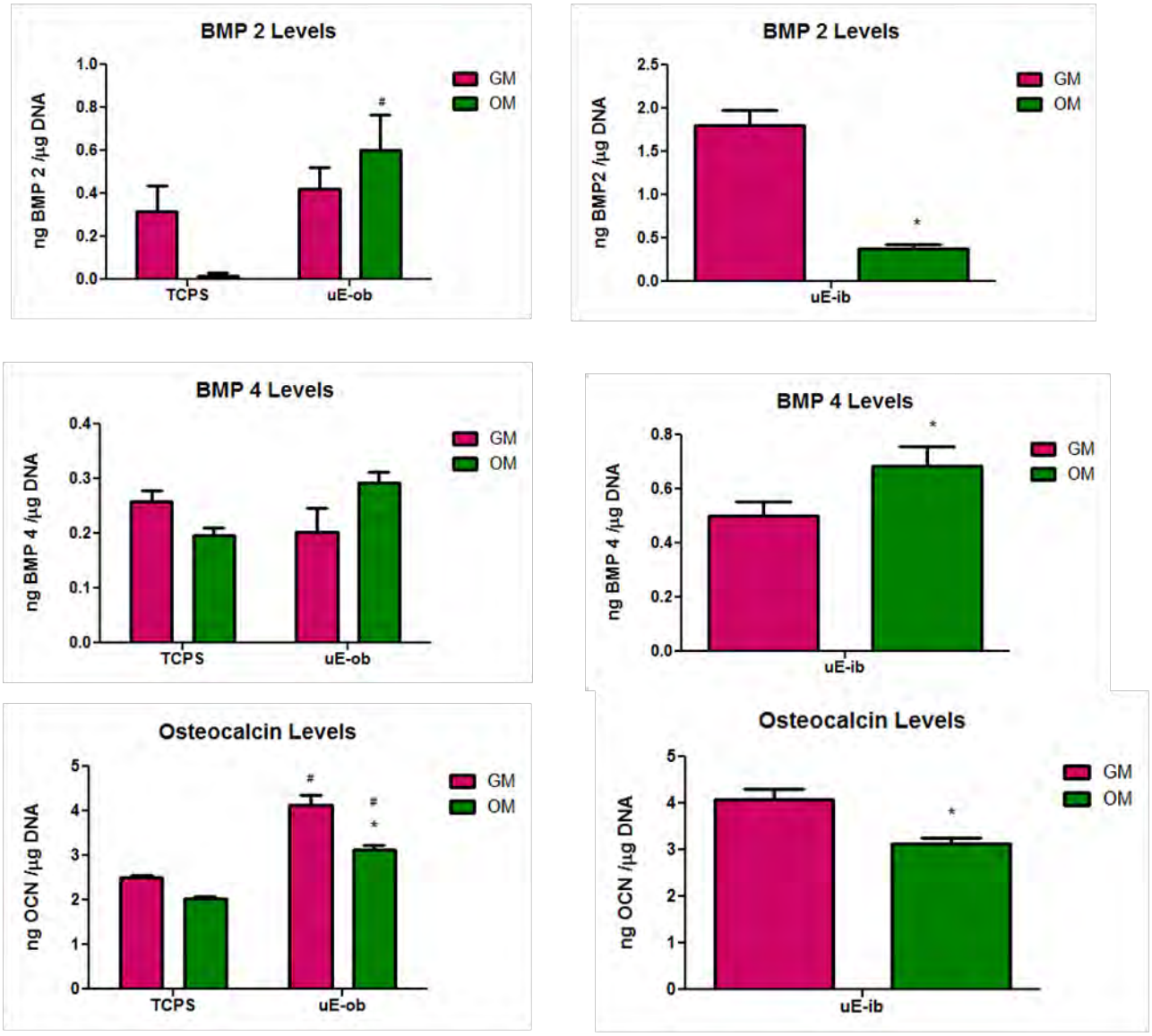

Figure 26. Osteogenic Local Factors produced by hASCs, TCPS (tissue culture polystyrene), uE-ob (microencapsulated – outside the beads), uE-ib (microencapsulated – inside the beads),* Significance compared to GM, $ significance compared to OM, % significance compared to liver, # compared to TCPS, @ compared to uE-ob.

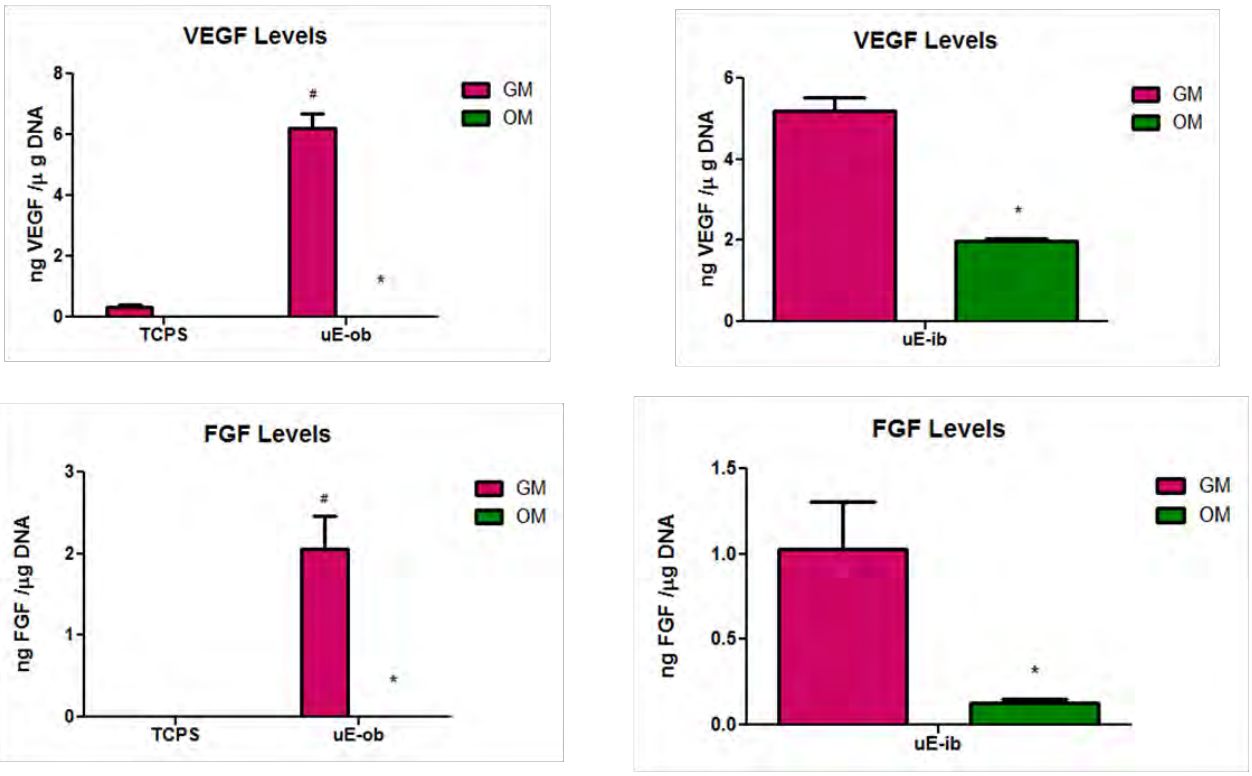

Figure 27 Angiogenic Factors produced by hASCs, TCPS (tissue culture polystyrene), uE-ob (microencapsulated – outside the beads), uE-ib (microencapsulated – inside the beads),* Significance compared to GM, $ significance compared to OM, % significance compared to liver, # compared to TCPS, @ compared to uE-ob.

REPORTABLE OUTCOMES

Publications end 2011-2012

1. Nair R, Ngangan AV, Kemp ML, McDevitt TC. Gene expression signatures of extracellular matrix and growth factors during embryonic stem cell differentiation, *re-submitted (PLoS ONE)*.
2. Ngangan AV, Waring JC, McDevitt TC. Soluble factors secreted by differentiating embryonic stem cells stimulate exogenous cell proliferation and migration, *submitted & in revision (J Cell Biochem)*.
3. Hermann CD, Richards MA, Olivares-Navarrete R, Williams JK, Guldberg RE,Skrinjar O, Schwartz Z, Boyan BD. Algorithm to assess cranial suture fusion with varying and discontinuous mineral density. Ann Biomed Eng. 2012 Jul;40(7):1597-609. Epub 2012 Feb 14. PubMed PMID: 22350663.
4. Erdman CP, Dosier CR, Olivares-Navarrete R, Baile C, Guldberg RE, Schwartz Z, Boyan BD. Effects of resveratrol on enrichment of adipose-derived stem cells and their differentiation to osteoblasts in two-and three-dimensional cultures. J Tissue Eng Regen Med. 2012 Mar 30. doi: 10.1002/term.513. [Epub ahead of print]PubMed PMID: 22467433.
5. Dosier CR, Erdman CP, Park JH, Schwartz Z, Boyan BD, Guldberg RE. Resveratrol effect on osteogenic differentiation of rat and human adipose derived stem cells in a 3-D

culture environment. J Mech Behav Biomed Mater. 2012 Jul;11:112-22. Epub 2011 Aug 31. PubMed PMID: 22658160; PubMed Central PMCID: PMC3367162.
6. Markowski MC, Brown AC, Barker TH. Directing epithelial to Mesenchymal transition through engineered microenvironments displaying orthogonal adhesive and mechanical cues. J Biomed Mater Res A. 2012 May 21. doi: 10.1002/jbm.a.34068.[Epub ahead of print] PubMed PMID: 22615133.
7. Huang X, Yang N, Fiore VF, Barker TH, Sun Y, Morris SW, Ding Q, Thannickal VJ,Zhou Y. Matrix Stiffness-Induced Myofibroblast Differentiation Is Mediated by Intrinsic Mechanotransduction. Am J Respir Cell Mol Biol. 2012 Mar 29. [Epub ahead of print] PubMed PMID: 22461426.
8. Stabenfeldt SE, Gourley M, Krishnan L, Hoying JB, Barker TH. Engineering fibrin polymers through engagement of alternative polymerization mechanisms. Biomaterials. 2012 Jan;33(2):535-44. Epub 2011 Oct 21. PubMed PMID: 22018389; PubMed Central PMCID: PMC3350801.
9. Stabenfeldt SE, Aboujamous NM, Soon AS, Barker TH. A new direction for anticoagulants: Inhibiting fibrin assembly with PEGylated fibrin knob mimics.Biotechnol Bioeng. 2011 Apr 21. doi: 10.1002/bit.23184. [Epub ahead of print]PubMed PMID: 21520023; PubMed Central PMCID: PMC3168719.
10. Barker TH. The role of ECM proteins and protein fragments in guiding cell behavior in regenerative medicine. Biomaterials. 2011 Jun;32(18):4211-4. PubMed PMID: 21515169.
11. Singh K, Moyer H, Williams JK, Schwartz Z, Boyan BD. Fibrin glue: a scaffold for cellular-based therapy in a critical-sized defect. Ann Plast Surg 2011 66:301-5.
12. Raines AL, Sunwoo M, Gertzman AA, Thacker K, Guldberg RE, Schwartz Z, boyan BD. Hyaluronic acid stimulates neovascularization during the regeneration of bone marrow after ablation. J Biomed Mater Res A 2011 96:575-83.
13. Boyan BD, Schwartz Z. Regenerative medicine. Are calcium phosphate ceramics “smart” materials? Nat Rev Rheumatol 2011 7:8-9.
14. Novotny SA, Warren GF, Lin AS Guldberg RE, Baltgalvis KA, Lowe DA. Bone is functionally impaired in dystrophic mice but less so than skeletal muscle. Neuromuscul Disord 2011 21:183-93.
15. Kolambkar YM, Dupont KM, Boerckel JD, Huebsch N, Mooney DJ, Hutmacher DW, Guldberg RE. An alginate-based hybrid system for growth factor delivery in the functional repair of large bone defects. Biomaterials 2011 32:65-74.
16. Lee CS, Chen J, Wang Y, Williams JK, Ranly DM, Schwartz Z, Boyan BD. Coordinated tether formation in anatomically distinct mice growth centers is dependent on a functional vitamin D receptor and is tightly linked to three-dimensional tissue morphology. Bone. 2011 May 11. PubMed PMID: 21601024.
17. Boerckel, J.D., Uhrig, B.A., Willett, N.J., Guldberg, R.E., "Mechanical Regulation of Vascular Growth and Tissue Regeneration In Vivo," Proceedings of the National Academies of Science, 108(37):E674-80, 2011.
18. Peister, A., Woodruff, M.A., Prince, J.J., Gray, D.P., Hutmacher, D.W., Guldberg, R.E., "Cell Sourcing for bone tissue engineering: Amniotic fluid stem cells have delayed robust differentiation compared to mesenchymal stem cells," Stem Cell Research, 7(1):17-27, 2011.
19. Boerckel, J., Kolambkar, Y., Dupont, K., Uhrig, B., Phelps, E., Stevens, H., Garcia, A.J., Guldberg, R.E., "Effects of Protein Dose and Delivery System on BMP-Mediated Bone Regeneration, " Biomaterials, ;32(22):5241-51, 2011.

Presentations 2011-2012

1. Lee CSD, Watkins EA, Burnsed OA, Willoiams JK, Schwartz Z, Boyan BD: Optimizing human adipose stem cells as trophic factor sources for cartilage regeneration, submitted to: Tissue Engineering International and Regenerative Medicine Society (TERMIS), Houston, TX, December 13-14, 2011.
2. Lee CSD, Watkins EA, Burnsed OA, Raghuram V, Schwartz Z, Boyan BD: Adipose stem cells secrete factors that inhibit cartilage regeneration, submitted to: Tissue Engineering International and Regenerative Medicine Society (TERMIS), Houston, TX, December 13-14, 2011.
3. Lee CSD, Watkins EA, Burnsed OA, Schwartz Z, Boyan BD: Chondrogenic media and microencapsulation is effective in tailoring adipose stem cell trophic factor expression regardless of anatomical site, passage, or donor age, submitted to: Tissue Engineering International and Regenerative Medicine Society (TERMIS), Houston, TX, December 13-14, 2011.
4. Hermann CD, Wilson S, Lawrence KA, Ning X, Olivares-Navarrete R, Williams JK, Murthy N, Schwartz Z, Boyan BD: Novel click-hydrogel therapy for juvenile murine model of re-synostosis, submitted to: Tissue Engineering International and Regenerative Medicine Society (TERMIS), Houston, TX, December 13-14, 2011.
5. Pan QF, Olivares-Navarrete R, Hyzy SL, Schwartz Z, Boyan BD: 24R,25dihydroxyvitamin D_3 prevents articular cartilage degradation induced by IL~1β: submitted to: Orthropaedic Research Society (ORS), San Francisco, CA, February 3-7, 2012.
6. Lee CSD, Watkins EA, Burnsed OA, Willoiams JK, Schwartz Z, Boyan BD: Optimizing human adipose stem cells as trophic factor sources for cartilage regeneration, submitted to: Orthropaedic Research Society (ORS), San Francisco, CA, February 3-7, 2012.
7. Lee CSD, Watkins EA, Burnsed OA, Raghuram V, Schwartz Z, Boyan BD: Adipose stem cells secrete factors that inhibit cartilage regeneration, submitted to: Orthropaedic Research Society (ORS), San Francisco, CA, February 3-7, 2012.
8. Burnsed OA, Olivares-Navarrete R, Hyzy SL, Schwartz Z, Boyan BD: Decellularized shark cartilage for promotion of chondrogenesis, submitted to: 16th Annual Hilton Head Workshop, Hilton Head, SC, March 14-17, 2012.
9. Wasilewski CE, Olivares-Navarrete R, Hyzy SL, Schwartz Z, Boyan BD: HIF1α inhibition in human adipose stem cells for promotion of chondrogenesis, submitted to: 16th Annual Hilton Head Workshop, Hilton Head, SC, March 14-17, 2012.
10. Herman CD, Lawrence K, Olivares-Navarrete R, Williams, JK, Schwartz Z, Boyan BD: Time course and gene expression analysis of juvenile mouse re-synosis, submitted to: American Association for Dental Research (AADR), Tampa, FL, March 21-24, 2012.
11. Lawrence K, Olivares-Navarrete R, Williams, JK, Schwartz Z, Boyan BD: Rapid re-synostosis in murine model is both location and age dependent, submitted to: American Association for Dental Research (AADR), Tampa, FL, March 21-24, 2012.
12. Boyan BD, Hermann CD, Lawrence K, Olivares-Navarrete R, Williams JK, Schwartz Z: Time course and gene expression analysis of infant mouse model of re-synostosis, submitted to: Plastic Surgery Research Council (PSRC), Ann Arbor, MI, June 14-17, 2012.
13. Lawrence K, Hermann CD, Olivares-Navarrete R, Williams JK, Schwartz Z, Boyan BD: Rapid re-synostosis in mice is both location and age dependent, submitted to: Plastic Surgery Research Council (PSRC), Ann Arbor, MI, June 14-17, 2012.
14. Pan Q, Boyan BD, Schwartz Z: 24R,25-Dihydroxy vitamin D_3 protects rat articular chondrocytes from degradation induced by IL-1β in vitro, submitted to: Vitamin D Workshop, Houston, TX, June 20-22, 2012.

15. Herman CD, Lawrence K, Wilson S, Xinghai N, Olivares-Navarrete R, Guldbert RE, Murthy N, Williams, JK, Schwartz Z, Boyan BD: Click-hydrogel therapy prevents re-synostosis in peadiatric mouse model, submitted to: International Association for Dental Research (IADR), Iquacu Falls, Brazil, June 20-23, 2012.
16. Wang Y, Foss C, Lotz E, Lee CSD, Migliaresi C, Schwartz Z, Boyan BD: Repair of critical size cartilage defects in rat xiphoid using adipose-derived stem cells and silk fibroin 3D porous scaffolds, submitted to: Tissue Engineering and Regenerative Medicine (TERMIS), Vienna, Austria, September 5-8, 2012.
17. Lee CSD, Watkins EA, Schwartz Z, Boyan BD: Chondrogenic medium components have distinct effects on growth factor production from adipose stem cells, submitted to: Tissue Engineering and Regenerative Medicine (TERMIS), Vienna, Austria, September 5-8, 2012.
18. Hermann CD, Lawrence K, Wilson S, Xinghai N, Olivares-Navarrete R, Guldbert RE, Murthy N, Williams, JK, Schwartz Z, Boyan BD: Click-hydrogel therapy prevents re-synostosis in peadiatric mouse model, submitted to: Tissue Engineering and Regenerative Medicine (TERMIS), Vienna, Austria, September 5-8, 2012.
19. Leslie S, Boyan BD, Schwartz Z: Injectable alginate hydrogels for stem cell delivery in bone regeneration applications, submitted to: Biomedical Engineering Society (BMES), Atlanta, GA, October 24-27, 2012.

CONCLUSIONS

- CABSS is on track with its proposed research tasks.
- The CABSS member company that licensed the patents received its first SBIR Phase I and Phase II.
- Relationships with industry sponsors has led to novel technologies, including decellularized allografts for cell delivery.
- Composite injuries remain a major challenge, therefore we are including a new project that will study muscle regeneration.

REFERENCES

1. Wang, Y., et al., *The synergistic effects of 3-D porous silk fibroin matrix scaffold properties and hydrodynamic environment in cartilage tissue regeneration.* Biomaterials, 2010. **31**(17): p. 4672-81.
2. Erdman CP, D.C., Olivares-Navarrete R, Baile C, Guldberg RE, Schwartz Z, Boyan BD., *Effects of resveratrol on enrichment of adipose-derived stem cells and their differentiation to osteoblasts in two-and three-dimensional cultures.* Journal of tissue engineering and regenerative medicine, 2012 **doi: 10.1002/term.513. [Epub ahead of print]**.

APPENDIX

1. CABSS RETREAT MINUTES
2. ACURO 10188001.01
3. ACURO 10188001.02
4. ACURO 10188001.03
5. ACURO 10188001.04
6. ACURO 10188001.05
7. HRPO APPROVAL

CABSS Retreat Minutes

Wednesday, January 11, 2012

Location: Parker H. Petit Institute for Bioengineering and Biosciences
Room #: 1128 – IBB Suddath Seminar Room
Address: 315 Ferst Drive, Atlanta, GA 30332
Attendees: Barbara Boyan, Mark Spilker, Gen Maria Britt, Franklin Bost, Joseph Williams, Linda Cendales (webinar), Zvi Schwartz, David Cohen, Gordon Warren, Todd McDevitt, Tom Barker, Robert Guldberg, Robert Christy, COL Michael Yaszemski (webinar), Michael Romanko, Kelvin Brockbank, Tim Patrick, Harold Shlevin, Dennis Hess, Rene Olivares-Navarrete, Chris Hermann and Maribel Baker.

8:00 a.m. **Breakfast: Welcome and Introduction** **Barbara D. Boyan**

Barbara Boyan, director of CABSS introduced the External Advisory Board members and guests. Following introductions she presented CABSS goals and current technologies.

The key for technology transfer lies in early partnership with industry. Georgia Tech is willing to work with companies to license patents and during the early stages of research.

Animal models are used as technology platforms to reduce time to the market. CABSS has several animal models that can be used to test devices and technology formulations.

The EAB was charged with three questions to discuss at the end of the meeting and provide feedback to CABSS investigators.

8:20 a.m. **ISR Research** **Robert Christy**

Bob Christy, Program Officer of CABSS, introduced the Institute for Surgical Research and its different areas of research.

Currently, extremities are the most commonly injured part of the body. CABSS has several projects concentrated in the extremities.

CABSS fits in the CRMRP: Clinical and Rehabilitation Medicine.

Other areas of research within ISR are: pain control, dental disease and trauma, dental and biomedical research, damage control resuscitation.

Damage control resuscitation currently uses tourniquets and hemostatic dressings to stop bleeding during combat. There is a need for more technological solutions to stop bleeding in these cases.

The dental group is currently working on a BioMASK that could use the superhydrophobic coating technology. They are also working on reducing biofilm from wound healing, and scar mitigation. CABSS can help with these areas of research.

Limitations of currently available FDA approved products

1) Availability of autologous epidermal cells, especially in case of extensive burn injuries.

2) Autologous epidermal cells require several weeks to expand and has a low rate of graft uptake (e.g. CEA).

3) Failure of graft integration due to poor vascularization and do not remain intact long term.

Why the proposed strategy will improve outcomes of severely injured soldiers

1) Adipose stem cells (ASCs) are **readily available, abundant** and can be easily manipulated without any added cytokine or growth inducers.

2) ASCs are sourced from an **individual patient** which results in an autograft with no immune complications.

3) ASCs can be used as a **single cell source to develop vascular**, dermal and epithelial cells providing a system for development of a vascularized skin equivalent.

4) The ASCs are induced to differentiate towards vascular and dermal cells via inherent properties of the scaffolds **with no drugs or growth factors**.

5) The formation of **blood vessels** within the matrices will **increase the viability and survival of the graf**t, thus facilitating its integration into both the burn and/or donor-site wound beds.

CABSS Investigators Progress Report

8:50 a.m. Cartilage Regeneration Barbara D. Boyan

Barbara presented results from the silk scaffold. This past year CABSS worked on finding the best formulation for cartilage regeneration. Great results were obtained in vitro but not in vivo. Therefore, they have decided to abandon this technology.

Since human articular chondrocytes do not preserve their phenotypes, they are looking at stem cells to regenerate to chondrocytes.

SpherIngenics, the spin-off company of CABSS is looking at regenerating cartilage with the microbead technology. Currently, growth factors are retained in the bead. The bead can be used as a time release agent, but controlled growth factor releasing over time.

The group is still working on the microbead degradation.

There are some osteoarthritis studies currently performed by the laboratory that showed that 24,25 vitamin D block apoptosis of cells. This treatment can be used as a therapeutic agent to treat osteoarthritis. They have made it work in vitro.

9:10 a.m. Wound Care: Acellular Therapies Derived from Stem Cells Todd McDevitt

Todd McDevitt, CABSS investigator, presented his current research on Embryoid body using pluripotent stem cells.

Their project is currently looking to see if you could remove the pluripotent cells from the Embryoid body and still get the same benefits.

This technology can have high density of cells, and keep them from agglomeration.

Decellularized embryoid bodies can retain their body shape without the cells on it.

An idea arose from the EAB that these natural matrices without the cells can be added to the microbeads and it will pass as a tissue product through the FDA.

Current animal studies with this embryoid body technology have shown positive results in dermal wound healing. Not sure if this is a result of contraction or increase wound healing rate. They are changing animal models to test for this.

The EBM and DBM showed similar levels for osteogenesis. Histology showed new bone remodeling. They received an R01 Transformative grant from NIH last September for this work.

9:30 a.m. Composite Models Robert E. Guldberg

Bob Guldberg, CABSS investigator, presented his current work on composite models.

Currently they have one of their technologies in Pre-clinical large animal studies in Australia. CABSS is partly funding for this study. Several companies are sponsoring this project with funds or products.

The BMP dose used in their hydrogel meshes are 1/25 of the current approved doses. Results with the mesh+hydrogel were better, and were able to sustain BMP delivery.

Muscle+Bone studies – muscle only partially recovers.

Stiff plate vs. Compliant plate studies – stiff plate + BMP was the only one that healed. Mechanical loading increased vascular diameter with compliant plate.

9:50 a.m. COFFEE BREAK

10:10 a.m. Internal Bleeding Detection Mechanism Ravi Bellamkonda

Due to schedule confusion, Dr. Bellamkonda was unable to present on this year's CABSS retreat.

10:30 a.m. Wound Stasis and Repair Thomas Barker

Tom Barker, CABSS investigator, presented his current work on fibrin peptides for wound healing.

His lab is trying to work with more clinically relevant knobs for wound healing. He is currently collaborating with Andrew Lyons using microgels as hemostatic agents that interact with fibrinogen. These microgels swell and can be used as a space filling entity. This can help slow down coagulation process.

Current formulations of knob-displaying microgels do NOT show promise as a rapid hemostat
- Next generation designs will include higher affinity binding ligands with specificity to fibrin protofibrils
- Possible new designs in structure of microgels
- Possible phase transition features

Current microgels do appear to be attractive modulators of fibrin matrices.
- Preliminary evidence suggest they may confer mechanical strength to fibrin gels derived from very dilute fibrinogen solutions
- Possible role in the development of strong yet permissive gels for enhanced tissue repair

10:50 a.m. Commercialization Efforts Barbara D. Boyan

CABSS currently is working with several companies which are sponsoring part of the large animal study conducted in Australia.

Carticept, Inc. has contributed hyaluronic acid for CABSS experiments.

MTF has donated tissues to test with our technologies.

We have expanded our efforts and affiliated with the following institutes and centers:

The Translational Research Institute for Biomedical Engineering and Science (TRIBES)

The Atlanta Pediatric Device Consortium (APDC) – FDA sponsored Center

The Center for Pediatric Healthcare Technology Innovation (CPHTI)

11:10 a.m. **POSTER SESSION: LUNCH BREAK**

New Project Ideas

12:30 p.m. **Superhydrophobic Coating** **Dennis Hess**
Rene Olivares Navarrete

The superhydrophobic coating was one of two new projects presented to the CABSS Advisory board as a possible project to be funded by CABSS.

Rene Olivares-Navarrete and Dennis Hess presented the technology. They are currently working on coating titanium surfaces and polymers for medical devices. Cells don't attach to superhydrophobic coating, nor bacteria. It can be used as an antibacterial coating.

An idea was brought up to use it in the Biomask project currently being worked by the ISR.

12:45 p.m. **Drug Delivery Hydrogel** **Chris Hermann**

Chris Hermann presented a new hydrogel that can be used as a delivery method for several medical applications. The technology is being researched to prevent re-synostosis. There are other applications to promote bone regeneration in non-unions and to prevent ankylosis.

1:00 p.m. **Advisory Board Closed Meeting** **David Cohen/**
Michael Yaszemski

2:00 p.m. **Future Strategic Plan**

1. Are the problems we are addressing relevant to military medical problems?

The advisory board agrees that CABSS is addressing medical problems relevant to the military.

2. Is our distribution of resources between discovery, early basic research, and translational research appropriate?

Maribel Baker will send a breakdown of the budgets and how much we are spending on each project. The advisory board suggested using the TRL metric to see how far along a project is and if it's going to be commercializable. Michael Romanko will be sending these metrics to Barbara Boyan.

3. Could we adapt our technology platforms to address emerging medical concerns for the military?

The advisory board suggested using the animal models that CABSS currently have and focus on using it on translating technologies using these models. Not investing more funds in new models, but taking advantage of the models we currently have.

CABSS had a meeting with SJTRI to discuss standardizing the animal models to be used for industry. SJTRI will apply for ASTM standards, and they are willing to give us 50% of the profit they made on using these animal models.

The advisory board sees the osteoarthritis project as very interesting. This will be a long term 10-15 year project. CABSS should concentrate on preventive technologies for osteoarthritis.

The advisory board was very enthusiastic over the superhydrophobic project. There are several other medical applications that can benefit from this coating.

Next year, the advisory board would like to see the TRL track system ahead of time to discuss the results during the CABSS meeting.

Adjourn

DEPARTMENT OF THE ARMY
US ARMY MEDICAL RESEARCH AND MATERIEL COMMAND
504 SCOTT STREET
FORT DETRICK, MD 21702-5012

REPLY TO
ATTENTION OF

June 02, 2011

Director, Office of Research Protections
Animal Care and Use Review Office

Subject: Review of USAMRMC Proposal Number 10188001, Award Number W81XWH-11-1-0306 entitled, "Advanced Bioengineering for Soldier Survivability"

Principal Investigator Barbara Boyan
Georgia Tech Research Corporation
Atlanta, GA

Dear Dr. Boyan:

Reference: (a) DOD Instruction 3216.01, "Use of Animals in DOD Programs"
(b) US Army Regulation 40-33, "The Care and Use of Laboratory Animals in DOD Programs"
(c) Animal Welfare Regulations (CFR Title 9, Chapter 1, Subchapter A, Parts 1-3)

The above-referenced proposal is “complex,” having multiple protocols associated with it under the same award. In accordance with the above references, the protocol/s listed below which is/are associated with proposal 10188001 is/are approved by the USAMRMC Animal Care and Use Review Office (ACURO) for the use of the specific species mentioned and will remain so until its modification, expiration or cancellation.

Protocol 10188001.01 entitled, "Non-Invasive Diagnosis of Internal Bleeding Using Iodinated Liposomal Nanocarriers," IACUC Protocol Number A11003, Principal Investigator Ravi Bellamkonda, is approved for the use of rats. This protocol was approved by the Georgia Institute of Technology IACUC.

When updates or changes occur, documentation of the following action or events must be forwarded immediately to ACURO:

- IACUC-approved modifications, suspensions, and triennial reviews of the protocol (All amendments or modifications to previously authorized animal studies must be reviewed and approved by the ACURO prior to initiation.)
- USDA annual program/facility inspection reports
- Reports to OLAW involving this protocol regarding

  a. any serious or continuing noncompliance with the PHS Policy;
  b. any serious deviation from the provisions of the Guide for the Care and Use of Laboratory Animals; or
  c. any suspension of this activity by the IACUC

- USDA or OLAW regulatory noncompliance evaluations of the animal facility or program
- AAALAC, International status change (gain or loss of accreditation only)

Throughout the life of the award, the awardee is required to submit animal usage data for inclusion in the DOD Annual Report on Animal Use. Please ensure that the following animal usage information is maintained for submission:

- Species used (must be approved by this office)
- Number of each species used
- USDA Pain Category for all animals used

For further assistance, please contact the Director, Animal Care and Use Review Office at (301) 619-2283, FAX (301) 619-4165, or via e-mail: acuro@amedd.army.mil.

Sincerely,

Alec Hail, DVM, DACLAM
Colonel, US Army
Director, Animal Care and
Use Review Office

Copies Furnished:
Mr. Lance Nowell, US Army Medical Research Acquisition Activity (USAMRAA)
Dr. Robert J. Christy, US Army Institute of Surgical Research (USAISR)
Dr. Jeffrey E. Stephenson/MCMR-ZB-PH
Ms. Maribel Baker, Georgia Institute of Technology
Ms. Anna Marie Lee, Georgia Institute of Technology
Dr. Ravi Bellamkonda, Georgia Tech Research Corporation

DEPARTMENT OF THE ARMY
US ARMY MEDICAL RESEARCH AND MATERIEL COMMAND
504 SCOTT STREET
FORT DETRICK, MD 21702-5012

REPLY TO
ATTENTION OF

May 12, 2011

Director, Office of Research Protections
Animal Care and Use Review Office

Subject: Review of USAMRMC Proposal Number 10188001 entitled, "Advanced Bioengineering for Soldier Survivability"

Principal Investigator Barbara Boyan
Georgia Tech Research Corporation
Atlanta, GA

Dear Dr. Boyan:

Reference: (a) DOD Instruction 3216.01, "Use of Animals in DOD Programs"
(b) US Army Regulation 40-33, "The Care and Use of Laboratory Animals in DOD Programs"
(c) Animal Welfare Regulations (CFR Title 9, Chapter 1, Subchapter A, Parts 1-3)

The above-referenced proposal is “complex,” having multiple protocols associated with it under the same award. In accordance with the above references, the protocol/s listed below which is/are associated with proposal 10188001 is/are approved by the USAMRMC Animal Care and Use Review Office (ACURO) for the use of the specific species mentioned and will remain so until its modification, expiration or cancellation.

Protocol 10188001.02 entitled, "Evaluation of Palate Graft Formulation to Enhance and Protect Implant Osseointegration," IACUC protocol number A10054, Principal Investigator Barbara Boyan, is approved for the use of rats. This protocol was approved by the Georgia Institute of Technology IACUC.

When updates or changes occur, documentation of the following action or events must be forwarded immediately to ACURO:

- IACUC-approved modifications, suspensions, and triennial reviews of the protocol (All amendments or modifications to previously authorized animal studies must be reviewed and approved by the ACURO prior to initiation.)
- USDA annual program/facility inspection reports
- Reports to OLAW involving this protocol regarding

  a. any serious or continuing noncompliance with the PHS Policy;
  b. any serious deviation from the provisions of the Guide for the Care and Use of Laboratory Animals; or
  c. any suspension of this activity by the IACUC

- USDA or OLAW regulatory noncompliance evaluations of the animal facility or program
- AAALAC, International status change (gain or loss of accreditation only)

Throughout the life of the award, the awardee is required to submit animal usage data for inclusion in the DOD Annual Report on Animal Use. Please ensure that the following animal usage information is maintained for submission:

- Species used (must be approved by this office)
- Number of each species used
- USDA Pain Category for all animals used

For further assistance, please contact the Director, Animal Care and Use Review Office at (301) 619-2283, FAX (301) 619-4165, or via e-mail: acuro@amedd.army.mil.

NOTE: Do not construe this correspondence as approval for any contract funding. Only the Contracting Officer or Grant Officer can authorize expenditure of funds. It is recommended that you contact the appropriate Contract Specialist or Contracting Officer regarding the expenditure of funds for your project.

Sincerely,

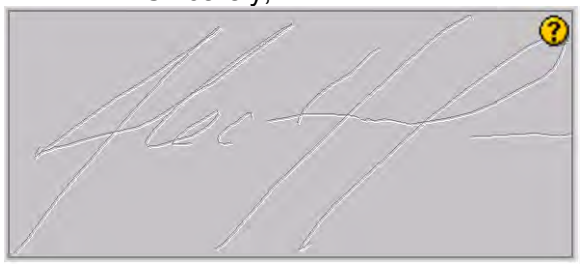

Alec Hail, DVM, DACLAM
Colonel, US Army
Director, Animal Care and
Use Review Office

Copies Furnished:
Dr. Robert J. Christy, US Army Institute of Surgical Research (USAISR)
Dr. Jeffrey E. Stephenson/MCMR-ZB-PH
Ms. Maribel Baker, Georgia Institute of Technology
Ms. Anna Marie Lee, Georgia Institute of Technology

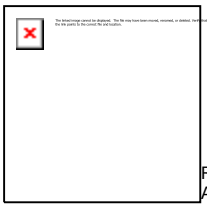

REPLY TO
ATTENTION OF

DEPARTMENT OF THE ARMY
US ARMY MEDICAL RESEARCH AND MATERIEL COMMAND
504 SCOTT STREET
FORT DETRICK, MD 21702-5012

January 19, 2012

Director, Office of Research Protections
Animal Care and Use Review Office

Subject: Review of USAMRMC Proposal Number 10188001, Award Number W81XWH-11-1-0306 entitled, "Advanced Bioengineering for Soldier Survivability"

Principal Investigator Barbara Boyan
Georgia Tech Research Corporation
Atlanta, GA

Dear Dr. Boyan:

Reference: (a) DOD Instruction 3216.01, "Use of Animals in DOD Programs"
(b) US Army Regulation 40-33, "The Care and Use of Laboratory Animals in DOD Programs"
(c) Animal Welfare Regulations (CFR Title 9, Chapter 1, Subchapter A, Parts 1-3)

The above-referenced proposal is “complex,” having multiple protocols associated with it under the same award. In accordance with the above references, the protocol/s listed below which is/are associated with proposal 10188001 is/are approved by the USAMRMC Animal Care and Use Review Office (ACURO) for the use of the specific species mentioned and will remain so until its modification, expiration or cancellation.

Protocol 10188001.03 entitled, "Development of a Rabbit Ear Defect Model for Cartilage Regeneration Strategies," IACUC protocol number A11079, Principal Investigator Barbara Boyan, is approved for the use of rabbits. This protocol was approved by the Georgia Institute of Technology IACUC.

When updates or changes occur, documentation of the following action or events must be forwarded immediately to ACURO:

- IACUC-approved modifications, suspensions, and triennial reviews of the protocol (All amendments or modifications to previously authorized animal studies must be reviewed and approved by the ACURO prior to initiation.)
- USDA annual program/facility inspection reports
- Reports to OLAW involving this protocol regarding

  a. any serious or continuing noncompliance with the PHS Policy;
  b. any serious deviation from the provisions of the Guide for the Care and Use of Laboratory Animals; or
  c. any suspension of this activity by the IACUC

- USDA or OLAW regulatory noncompliance evaluations of the animal facility or program
- AAALAC, International status change (gain or loss of accreditation only)

Throughout the life of the award, the awardee is required to submit animal usage data for inclusion in the DOD Annual Report on Animal Use. Please ensure that the following animal usage information is maintained for submission:

- Species used (must be approved by this office)
- Number of each species used
- USDA Pain Category for all animals used

For further assistance, please contact the Director, Animal Care and Use Review Office at (301) 619-2283, FAX (301) 619-4165, or via e-mail: acuro@amedd.army.mil.

Sincerely,

For 

James Sheets, DVM, DACLAM
Colonel, US Army
Director, Animal Care and
Use Review Office

Copies Furnished:
Lance Nowell, US Army Medical Research Acquisition Activity (USAMRAA)
Dr. Robert J. Christy, US Army Institute of Surgical Research (USAISR)
Dr. Jeffrey E. Stephenson/MCMR-ZB-PH
Ms. Maribel Baker, Georgia Institute of Technology
Ms. Anna Marie Lee, Georgia Institute of Technology

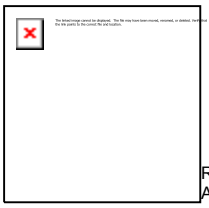

REPLY TO
ATTENTION OF

DEPARTMENT OF THE ARMY
US ARMY MEDICAL RESEARCH AND MATERIEL COMMAND
504 SCOTT STREET
FORT DETRICK, MD 21702-5012

January 13, 2012

Director, Office of Research Protections
Animal Care and Use Review Office

Subject: Review of USAMRMC Proposal Number 10188001, Award Number W81XWH-11-1-0306 entitled, "Advanced Bioengineering for Soldier Survivability"

Principal Investigator Barbara Boyan
Georgia Tech Research Corporation
Atlanta, GA

Dear Dr. Boyan:

Reference: (a) DOD Instruction 3216.01, "Use of Animals in DOD Programs"
(b) US Army Regulation 40-33, "The Care and Use of Laboratory Animals in DOD Programs"
(c) Animal Welfare Regulations (CFR Title 9, Chapter 1, Subchapter A, Parts 1-3)

The above-referenced proposal is “complex,” having multiple protocols associated with it under the same award. In accordance with the above references, the protocol/s listed below which is/are associated with proposal 10188001 is/are approved by the USAMRMC Animal Care and Use Review Office (ACURO) for the use of the specific species mentioned and will remain so until its modification, expiration or cancellation.

Protocol 10188001.04 entitled, "Creation of a Rat Palate Defect Model to Evaluate Tissue Repair Strategies," IACUC protocol number A11080, Principal Investigator Barbara Boyan, is approved for the use of rats. This protocol was approved by the Georgia Institute of Technology IACUC.

When updates or changes occur, documentation of the following action or events must be forwarded immediately to ACURO:

- IACUC-approved modifications, suspensions, and triennial reviews of the protocol (All amendments or modifications to previously authorized animal studies must be reviewed and approved by the ACURO prior to initiation.)
- USDA annual program/facility inspection reports
- Reports to OLAW involving this protocol regarding

  a. any serious or continuing noncompliance with the PHS Policy;
  b. any serious deviation from the provisions of the Guide for the Care and Use of Laboratory Animals; or
  c. any suspension of this activity by the IACUC

- USDA or OLAW regulatory noncompliance evaluations of the animal facility or program
- AAALAC, International status change (gain or loss of accreditation only)

Throughout the life of the award, the awardee is required to submit animal usage data for inclusion in the DOD Annual Report on Animal Use. Please ensure that the following animal usage information is maintained for submission:

- Species used (must be approved by this office)
- Number of each species used
- USDA Pain Category for all animals used

For further assistance, please contact the Director, Animal Care and Use Review Office at (301) 619-2283, FAX (301) 619-4165, or via e-mail: acuro@amedd.army.mil.

Sincerely,

For 

James Sheets, DVM, DACLAM
Colonel, US Army
Director, Animal Care and
Use Review Office

Copies Furnished:
Lance Nowell, US Army Medical Research Acquisition Activity (USAMRAA)
Dr. Robert J. Christy, US Army Institute of Surgical Research (USAISR)
Dr. Jeffrey E. Stephenson/MCMR-ZB-PH
Ms. Maribel Baker, Georgia Institute of Technology
Ms. Anna Marie Lee, Georgia Institute of Technology

Zimbra mbaker38@mail.gatech.edu

+ Font Size -

A-16560.2, HRPO Approval Memorandum (Proposal Log Number 1018801, Award Number W81XWH-11-1-0306) (UNCLASSIFIED)

From : Caryn L Ms CIV USA MEDCOM USAMRMC Duchesneau <Caryn.Duchesneau@us.army.mil> Thu, Sep 08, 2011 05:33 PM

Subject : A-16560.2, HRPO Approval Memorandum (Proposal Log Number 1018801, Award Number W81XWH-11-1-0306) (UNCLASSIFIED)

To : 'barbara.boyan@bme.gatech.edu' <barbara.boyan@bme.gatech.edu>

Cc : Laura R Dr CIV USA MEDCOM USAMRMC Brosch <Laura.Brosch@us.army.mil>, Caryn L Ms CIV USA MEDCOM USAMRMC Duchesneau <Caryn.Duchesneau@us.army.mil>, Robert J Dr CIV USA MEDCOM AISR Christy <Robert.Christy@us.army.mil>, Lance Mr CIV USA MEDCOM USAMRAA Nowell <lance.nowell@us.army.mil>, Jodi H Ms CIV USA MEDCOM USAMRMC Bennett <Jodi.Bennett@us.army.mil>, 'srusche@atlplastic.com' <srusche@atlplastic.com>, 'kelly.winn@gtrc.gatech.edu' <kelly.winn@gtrc.gatech.edu>, 'Lucy.Yarbrough@osp.gatech.edu' <Lucy.Yarbrough@osp.gatech.edu>, Kristen R Ms CTR US USA MEDCOM USAMRMC Katopol <Kristen.Katopol@us.army.mil>, 'maribel.baker@bme.gatech.edu' <maribel.baker@bme.gatech.edu>, 'jwilliams@atlplastic.com' <jwilliams@atlplastic.com>, 'jeffrey.stephenson@tatrc.org' <jeffrey.stephenson@tatrc.org>, Susan E Ms CTR US USA MEDCOM USAMRMC Kitchen <Susan.Kitchen@us.army.mil>

Classification: UNCLASSIFIED Caveats: NONE

SUBJECT: Initial Approval for the Protocol, "Development of Human Cartilage Preservation," Submitted by Barbara D. Boyan, PhD, Georgia Tech Research Corporation, Atlanta, Georgia, in Support of the Proposal, "Advanced Bioengineering for Soldier Survivability," Submitted by Barbara D. Boyan, PhD, Georgia Tech Research Corporation, Atlanta, Georgia, Proposal Log Number 1018801, Award Number W81XWH-11-1-0306, HRPO Log Number A-16560.2

1. The subject protocol (version 19 July 2011) was approved by the Georgia Tech Research Corporation Institutional Review Board (IRB) on 6 September 2011. This protocol was reviewed by the U.S. Army Medical Research and Materiel Command (USAMRMC), Office of Research Protections (ORP), Human Research Protection Office (HRPO) and found to comply with applicable DOD, U.S. Army and USAMRMC human subjects' protection requirements. Please note: this approval addresses only the Georgia Tech Research Corporation.

2. This no greater than minimal risk study is approved for accrual of 20 human subject's samples acquired from The Children's Hospital of Atlanta.

3. The following are reporting requirements and responsibilities of the Principal Investigator to the HRPO. Failure to comply could result in suspension of funding.

a. Major modifications to the research protocol and any modifications that could potentially increase risk to subjects must be submitted to the HRPO for approval prior to implementation. Major modifications include a change in Principal Investigator, change or addition of an institution, elimination or alteration of the consent process, change in age range or change in/addition to the study population, or a change that could potentially increase risks to subjects.

b. All unanticipated problems involving risk to subjects or others must be promptly reported by telephone (301-619-2165), by email (hrpo@amedd.army.mil), or by facsimile (301-619-7803) to the HRPO. A complete written report will follow the initial notification. In addition to the methods above, the complete report can be sent to the U.S. Army Medical Research and Materiel Command, ATTN: MCMR-RP, 504 Scott Street, Fort Detrick, Maryland 21702-5012.

c. Suspensions, clinical holds (voluntary or involuntary), or terminations of this research by the IRB, the institution, the sponsor, or regulatory agencies will be promptly reported to the USAMRMC ORP HRPO.

d. Any deviation to the protocol that may have an adverse effect on the safety or rights of the subject or the integrity of the study must be reported to the HRPO as soon as the deviation is identified.

e. A copy of the continuing review approval notification by the Georgia Tech Research Corporation IRB must be submitted to the HRPO as soon as possible after receipt of approval. According to our records, it appears the next continuing review by the Georgia Tech Research Corporation IRB is due no later 3 August 2012. Please note that the HRPO also conducts random audits at the time of continuing review and additional information and documentation may be requested at that time.

f. The final study report submitted to the Georgia Tech Research Corporation IRB, including a copy of any acknowledgement documentation and any supporting documents, must be submitted to the HRPO as soon as all documents become available.

g. The knowledge of any pending compliance inspection/visit by the Food and Drug Administration (FDA), Office for Human Research Protections, or other government agency concerning this clinical investigation or research; the issuance of inspection reports, FDA Form 483, warning letters, or actions taken by any regulatory agencies including legal or medical actions; and any instances of serious or continuing noncompliance with the regulations or requirements must be reported immediately to the HRPO.

4. Please Note: The USAMRMC ORP HRPO conducts random site visits as part of its responsibility for compliance oversight. Accurate and complete study records must be maintained and made available to representatives of the USAMRMC as a part of their responsibility to protect human subjects in research. Research records must be stored in a confidential manner so as to protect the confidentiality of subject information.

5. Do not construe this correspondence as approval for any contract funding. Only the Contracting Officer or Grants Officer can authorize expenditure of funds. It is recommended that you contact the appropriate contract specialist or contracting officer regarding the expenditure of funds for your project.

6. The HRPO point of contact for this study is Susan Kitchen, BS, Human Subjects Protection Scientist, at 301-619-1126/susan.kitchen@us.army.mil.

CARYN L. DUCHESNEAU, CIP
Chief, Human Subjects Protection Review
Human Research Protection Office
Office of Research Protections
U.S. Army Medical Research and Materiel Command

Note: The official copy of this approval memo is housed with the protocol file at the Office of Research Protections, Human Research Protection Office, 504 Scott Street, Fort Detrick, MD 21702. Signed copies will be provided upon request.
Classification: UNCLASSIFIED Caveats: NONE